Density Functional (DFT) Study of the Anti−Syn Isomerization of the Butenyl Group in Cationic and Neutral (Butenyl)(butadiene)(monoligand)nickel(II) Complexes

Sven Tobisch*,† and Rudolf Taube‡

Institut für Physikalische Chemie der Martin-Luther-Universität Halle-Wittenberg, Fachbereich Chemie (Merseburg), D-06099 Halle, Germany, and Anorganisch-Chemisches Institut der Technischen Universität München, Lichtenbergstrasse 4, D-85747 Garching, Germany

Received December 21, 1998

The transition-metal assisted isomerization of the butenyl group, which most likely takes place via $\pi \rightarrow \sigma$ butenyl conversion followed by internal rotation around the C^2-C^3 single bond, was studied theoretically. This was performed using the density functional theory (DFT) with cationic and neutral (butenyl)(butadiene)(monoligand)nickel(II) complexes. The important structural accommodation during the process of rotational isomerism is the pyramidalization of the carbon center associated with sp^3 hybridization. There are two conformers of the rotational transition structure for the inward and outward rotation of the electron pair which is formed during the rotation. The $\pi \rightarrow \sigma$ butenyl conversion followed by formation of the rotational transition structure is accompanied by negative charge migration, which is mainly located at the rotated sp^3 carbon atom. The isomerization barrier is strongly influenced by the ligand's donor−acceptor ability. Our calculations indicate an increased barrier due to an α-alkyl substitution of the butenyl group. The σ-butenyl rotational transition structure is stabilized by the occupation of its single vacant coordination site by an additional ligand, which therefore gives rise to lower activation energy for isomerization.

Introduction

The stereospecific polymerization of butadiene mediated by Ziegler−Natta-type[1] catalysts is a technically important catalytic reaction.[2] From a mechanistic point of view, the diene polymerization, as a chemo-, regio-, and stereoselective C−C bond formation, is of fundamental importance. 1,3-Diene polymerization is an insertion polymerization,[3] as is that of mono-alkene; that is, the chain propagation occurs by monomer insertion into the metal−carbon bond. The main difference between 1-alkene and 1,3-dienes is that for 1-alkene the metal−carbon bond is of σ-type, while in the diene polymerization it is of the allylic π-type. Insertion of butadiene into the metal−carbon bond gives rise to a metal−butenyl bond. Butenyl−transition-metal−butadiene complexes have been experimentally verified as the active catalyst complexes.[4]

Concerning the insertion of butadiene into the butenyl−transition-metal bond two different mechanisms are proposed. Cossee and Arlman[5] first suggested that the η^2- or η^4-coordinated butadiene could be nucleophilically attacked by the butenyl end group in its η^1-coordination. In contrast to this σ-allyl-insertion mechanism, the butenyl group may also react with butadiene in its η^3-state; i.e., both reacting moieties are in π-coordination. This π-allyl-insertion mechanism was introduced by Taube et al.[6] In previous theoretical studies[7] we were able to show that the insertion of butadiene into the allylnickel(II) bond is energetically feasible within the π-coordination of the reacting parts.

* Corresponding author. E-mail: tobisch@chemie.uni-halle.de.
† Martin-Luther-Universität Halle-Wittenberg
‡ Technische Universität München.

(1) (a) Ziegler, K. *Angew. Chem.* **1964**, *76*, 545. (b) Natta, G. *Angew. Chem.* **1964**, *76*, 553.

(2) (a) *Applied Homogeneous Catalysis with Organometallic Complexes*; Cornils, B., Herrmann, W. A., Eds.; VCH: Weinheim, Germany, 1996. (b) Porri, L.; Giarrusso, A. In *Comprehensive Polymer Science*; Eastmond, G. C., Ledwith, A., Russo, S., Sigwalt, B., Eds.; Pergamon, Oxford, UK, 1989; Vol. 4, Part II, pp 53−108.

(3) Pino, P.; Giannini U.; Porri, L. In *Encyclopedia of Polymer Science and Engineering*, 2nd ed.; J. Wiley and Sons, New York, 1987; Vol. 8, pp 147−220.

(4) (a) Wilke, G.; Bogdanovic, B.; Hardt, P.; Heimbach, P.; Keim, W.; Kröner, M.; Oberkirch, W.; Tanaka, K.; Steinrücke, E.; Walter, D.; Zimmermann, H. *Angew. Chem., Int. Ed. Engl.* **1966**, *5*, 151. (b) Natta, G.; Porri, L.; Carbonaro, A.; Greco, A. *Makromol. Chem.* **1964**, *71*, 207. (c) Babitskii, B. D.; Dogoplosk, B. A.; Kormer, V. A.; Lobach, M. I.; Tinyakova, I. E.; Yakolev, V. A. *Isv. Akad. Nauk SSSR, Ser. Chem.* **1965**, 1507.

(5) (a) Cossee, P. In *Stereochemistry of Macromolecules*; Ketley A. D., Ed.; Marcel Dekker, Inc.: New York, **1967**; Vol. 1, p 145. (b) Arlman, E. J. *J. Catal.* **1966**, *5*, 178.

(6) (a) Taube, R.; Gehrke, J.-P.; Radeglia, R. J. *Organomet. Chem.* **1985**, *291*, 101. (b) Taube, R.; Gehrke, J.-P.; Böhme, P. *Wiss. Zeitschr. TH Leuna-Merseburg* **1987**, *39*, 310. (c) Sieler, J.; Kempe R.; Wache, S.; Taube, R. *J. Organomet. Chem.* **1993**, *455*, 241. (d) Taube, R.; Wache, S.; Sieler, J.; Kempe, R. *J. Organomet. Chem.* **1993**, *456*, 131. (e) Taube, R.; Schmidt, U.; Gehrke, J.-P.; Böhme, P.; Langlotz, J; Wache, S. *Makromol. Chem., Macromol. Symp.* **1993**, *66*, 245. (f) Taube, R.; Windisch, H.; Maiwald, S. *Makromol. Chem., Macromol. Symp.* **1995**, *89*, 393. (g) Taube, R.; Sylvester, G. In *Applied Homogeneous Catalysis with Organometallic Complexes*; Cornils, B., Herrmann, W. A., Eds.; VCH: Weinheim, Germany, 1996; pp 280−317.

(7) (a) Tobisch, S.; Bögel, H.; Taube, R. *Organometallics* **1998**, *17*, 1177. (b) Tobisch, S.; Bögel, H.; Taube, R. *Organometallics* **1996**, *15*, 3563.

10.1021/om9810302 CCC: $18.00
Publication on Web 07/17/1999

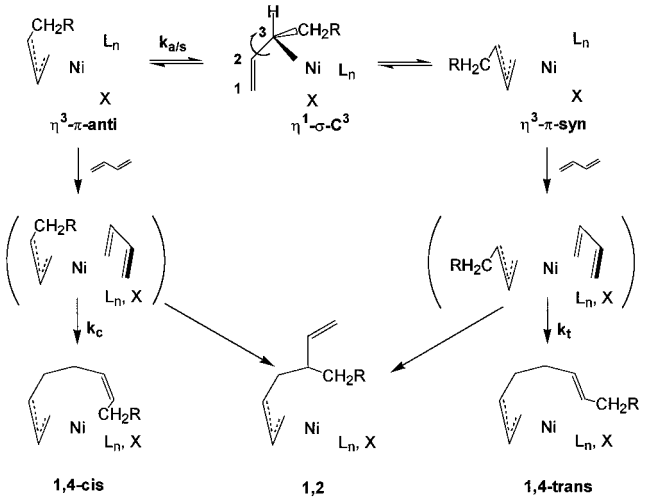

Figure 1. C−C bond formation in butenyl(butadiene)-(ligand)metal complexes in accordance with the anti-cis and syn-trans correlation.

The butenyl−transition-metal bond can exist in two isomeric forms, anti and syn,[8] which are in a structure dependent equilibrium (cf. Figure 1). According to the principle of least-structure variation and the anti-cis and syn-trans correlation[2] the butadiene insertion gives rise to a cis (k_c) or trans (k_t) double bond in the growing polymer chain extended by a newly formed C_4-unit when starting from an *anti*- or *syn*-butenyl group (cf. Figure 1).

To elucidate the mechanism of cis−trans regulation, two different processes and their relative rates must be interrelated. Those are the butadiene insertion and the anti−syn isomerization. In principle, two different cases can be distinguished, except for nearly identical rates of both processes. First, the conformational interconversion via anti−syn isomerization is much more rapid than the insertion of butadiene ($k_{a/s} \gg k_t$, k_c) and secondly, the reverse case is valid (k_t, $k_c \gg k_{a/s}$). Concerning the first case, which is a typical Curtin−Hammett situation, on account of the Curtin−Hammett principle[9] the position of the pre-established anti−syn equilibrium may not be relevant to the stereoselectivity attained by butadiene insertion. The cis−trans selectivity is determined solely by the difference in the free enthalpies between the competing transition states for butadiene insertion of both of the *anti*- and *syn*-butenyl forms. In the other case, a non-Curtin−Hammett situation with the rate of anti−syn isomerization is relatively low, the cis−trans selectivity may be determined by the formation of the *anti*- or the *syn*-butenyl structure in the catalyst complex, irrespective of the reactivity of the different butenyl forms (i.e., the difference in the free enthalpies of the corresponding transition states).

Although several mechanisms have been proposed,[10] the anti−syn isomerization in the η^3-π-coordinated butenyl group is very likely proceeding through an η^1-σ-butenyl intermediate, i.e., via $\pi \rightarrow \sigma$ or $\eta^3 \rightarrow \eta^1$ conversion, which has been proven by NMR spectroscopy on several transition metal complexes.[10] To accomplish anti−syn isomerization the $\pi \rightarrow \sigma$ butenyl group conversion must lead to an σ-C^3-butenyl intermediate followed by rotation of the vinyl group around the C^2-C^3 single bond (cf. Figure 2, course A). The alternative formed σ-C^1-butenyl intermediate also gives rise to a free rotating C−C single bond, but in contrast to the σ-C^3 structure, the butenyl group's configuration cannot be altered by internal rotation. In case of an unsubstituted π-allyl group the internal rotation within the σ-allyl intermediate yields an $1\text{-}H_{anti} \leftrightarrow 1\text{-}H_{syn}$ exchange of proton positions. For the butenyl anion the internal rotation around C^2-C^3 can occur in two different ways, i.e., via outward (TS-A) and inward (TS-B) rotation of the electron pair that is formed during the rotation (cf. Figure 2, course A). Without rotation around the $Ni-C^3$ σ-bond the isomerization gives rise to a change in the orientation of the butenyl group from supine to prone[11] (with C^1, C^3 pointing toward or away from the axial ligand, respectively, cf. Figure 2). The butenyl group's orientation is preserved if an additional rotation around the $Ni-C^3$ σ-bond takes place in the σ-C^3-butenyl intermediate (cf. Figure 2, schematically sketched by course A′).

Despite of its fundamental importance for the understanding of the cis−trans regulation of the butadiene polymerization, to date, no theoretical study employing reliable nonempirical methods has been carried out concerning the transition-metal assisted isomerization of the butenyl group. In the present study the anti−syn isomerization of the butenyl group will be explored theoretically on cationic and neutral (butenyl)(butadiene)(monoligand)nickel(II) complexes. We report the calculated geometries and Gibbs free energies of relevant structures of the isomerization process; i.e., the η^3-π *syn*- and *anti*-butenyl reactants and products and the η^1-σ-C^3 transition states. For each of the reactants, transition states, and products a number of conformers are possible, which were carefully explored. However, only the most stable conformers for each of them are given. Those represent the key structures that were passed through along the minimum energy pathway, provided that for the η^1-σ-C^3 intermediates the internal rotation around the $Ni-C^3$ σ-bond is energetically more feasible than that around the C^2-C^3 σ-bond. That will be confirmed for the [bis(allyl)-Ni-PMe_3] complex (section B) and also for the [(crotyl)(butadiene)(ethylene)-Ni-PMe_3]$^+$ complex (section E).

In our previous study[7a] on the whole polymerization cycle for the cationic and neutral butenyl(monoligand)-(butadiene)nickel(II) complexes the attention was focused on the σ-C^3 intermediates, which can be regarded as the precursors of the isomerization transition states.

(8) Syn refers to E and anti to Z skeletal geometry of the butenyl group.

(9) Seemann, J. I. *Chem. Rev.* **1983**, *83*, 83.

(10) (a) Vrieze, K. Fluxional allyl complexes. In *Dynamic Nuclear Magnetic Resonance Spectroscopy*: Jackman, L.M., Cotton, F.A., Eds.; Academic Press: New York, 1975. (b) Cotton, F. A.; Faller, J. W.; Musco, A. *Inorg. Chem.* **1967**, *6*, 179. (c) Vrieze, K.; Praat, A. P.; Cossee, P. *J. Organomet. Chem.* **1968**, *12*, 533. (d) Faller, J. W.; Incorvia, M. J.; Thomsen, M. E. *J. Am. Chem. Soc.* **1969**, *91*, 518. (e) Faller, J. W.; Thomsen, M. E.; Mattina, M. J. *J. Am. Chem. Soc.* **1971**, *93*, 2642. (f) Faller, J. W. *J. Organomet. Chem.* **1980**, *187*, 227. (g) Zschunke, A.; Nehls, I.; Meyer, H. *J. Organomet. Chem.* **1981**, *222*, 353. (h) Zschunke, A; Meyer, H.; Nehls, I. *Z. Anorg. Allg. Chem.* **1982**, *494*, 189. (i) Meyer, H.; Zschunke, A. *J. Organomet. Chem.* **1984**, *269*, 209. (j) Hoffmann, E. G.; Kallweit, R.; Schroth, G; Seevogel, K.; Stempfle, W.; Wilke, G. *J. Organomet. Chem.* **1975**, *97*, 183. (k) Powell, J.; Shaw, B. L. *J. Chem. Soc. (A)* **1967**, 1839. (l) van Leeuwen, P. W. N. M.; Praat, A. P. *J. Organomet. Chem.* **1970**, *21*, 501. (m) Hughes, R. P.; Powell, J. *J. Organomet. Chem.* **1973**, *60*, 387.

(11) Yasuda, H.; Nakamura, A. *Angew. Chem.* **1987**, *99*, 745.

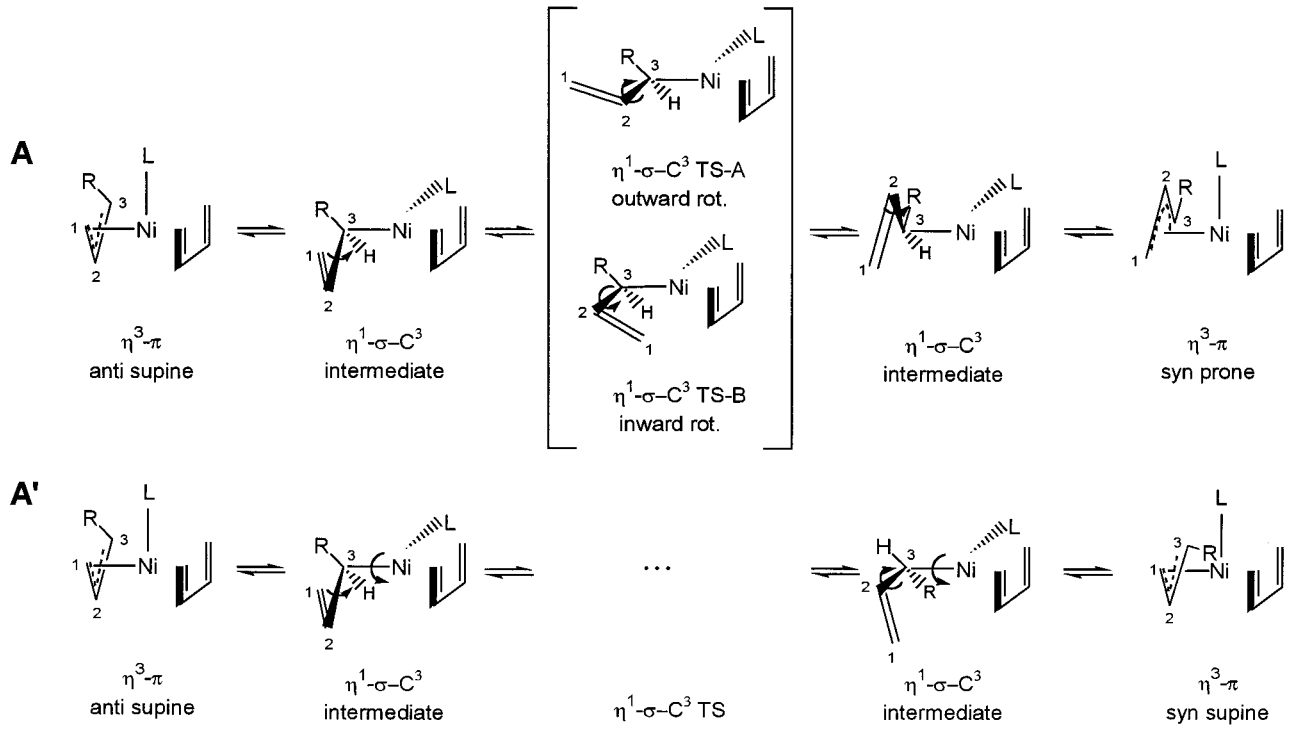

Figure 2. Proposed mechanism of butenyl group's isomerization in (butenyl)(butadiene)(monoligand)Ni(II) complexes.

In the present study the real rotational transition state structures are reported, which were confirmed to have only one imaginary frequency. The corresponding normal mode represents a rotational displacement along the C^2-C^3 bond.

We intend to present a comprehensive analysis of the influence of the transition metal (i.e., Ni(II) with a d^8-configuration), the donor−acceptor ability of the neutral and anionic ligand L and X, and the methyl substitution of the butenyl group at the terminal C^3 atom, that is involved in the rotation, on the isomerization barrier. The paper is therefore organized as follows. First, the rotational isomerism is examined for the free allyl and crotyl anions and the results are compared with available theoretical data from the literature (section A). In order to get an idea of the reliability of the chosen computational approach, the rotational automerism in the experimentally well investigated [bis(allyl)-Ni-PMe_3] complex is investigated by varying the basis set and DFT-Hamiltonian employed (section B). Subsequently, the results of the research of the anti−syn isomerization in cationic and neutral $[(allyl)(butadiene)\text{-}Ni^{II}\text{-}L/X]^{(+)}$ complexes and $[(crotyl)(butadiene)\text{-}Ni^{II}\text{-}L/X]^{(+)}$ complexes are reported (sections C and D, respectively). Finally, the influence of an additional ligand, which may occupy the single vacant site at the metal center that arises during the isomerization process, is explored for cationic and neutral $[(crotyl)(butadiene)(ethylene)\text{-}Ni^{II}\text{-}L/X]^{(+)}$ complexes, where ethylene serves as a simplified model of a coordinated double bond from the growing polybutadienyl chain (section E).

For the neutral ligand L = PF_3, PH_3, PMe_3, and C_2H_4 are chosen, whereas the iodine anion is adopted as a realistic anionic ligand X. In a recent theoretical study of $Fe(CO)_4$-PR_3 complexes,[12] the donor−acceptor ability of different organophosphorus ligands has been examined in detail. Following this study, all PR_3 ligands studied are essentially σ-donor ligands. Concerning the ligands considered in the present study, the donor strength increases in the order $PF_3 < PH_3 < PMe_3$. Only for the PF_3 has a noticeable π-back-donation contribution to the entire bonding interaction been observed.[12] We consider the different σ-donor ability of PR_3 ligands, which is related to their basicity, as the driving force that may influence the isomerization barrier height. The iodine anion act as a pure donor, but on the other hand, ethylene exhibits a bivalent electronic character. Ethylene can be a donor to a certain degree; however, in many cases this is surpassed by a greater acceptor ability.

Computational Details

The approximate density functional (DFT) calculations reported here were performed by using the DGauss program within the UniChem software environment[13] and the program package TURBOMOLE,[14] developed by Ahlrichs et al. at the University of Karlsruhe.

All calculations were carried out using the LDA with Slater's exchange functional[15a,b] and Vosko−Wilk−Nusair parameter-

(12) Gonzalez-Blanco, O.; Branchadell, V. *Organometallics* **1997**, *16*, 5556.

(13) (a) Andzelm, J.; Wimmer, E. *Physica B* **1991**, *172*, 307. (b) Andzelm, J. In *Density Functional Methods in Chemistry*; Labanowski, J.; Andzelm, J., Eds.; Springer: Berlin, 1991. DGauss and UniChem are software packages available from Molecular Simulations Inc.

(14) (a) Häser, M.; Ahlrichs, R. *J. Comput. Chem.* **1989**, *10*, 104. (b) Ahlrichs, R.; Bär, M.; Häser, M.; Horn, H.; Kölmel, C. *Chem. Phys. Lett.* **1989**, *162*, 165.

(15) (a) Dirac, P. A. M. *Proc. Cambridge Philos. Soc.* **1930**, *26*, 376. (b) Slater, J. C. *Phys. Rev.* **1951**, *81*, 385. (c) Vosko, S. H.; Wilk, L.; Nussiar, M. *Can. J. Phys.* **1980**, *58*, 1200. (d) Becke, A. D. *Phys. Rev.* **1988**, *A38*, 3098. (e) Perdew, J. P. *Phys. Rev.* **1986**, *B33*, 8822. (f) Lee, C.; Yang, W.; Parr, R. G. *Phys. Rev.* **1988**, *B37*, 785. (g) Miehlich, B.; Savin, A.; Stoll, H.; Preuss, H. *Chem. Phys. Lett.* **1989**, *157*, 200. (h) Becke, A. D. *J. Chem. Phys.* **1993**, *98*, 5648. (i) Becke, A. D. *J. Chem. Phys.* **1993**, *98*, 1372. (j) Perdew, J. P.; Wang, Y. *Phys. Rev.* **1992**, *B45*, 13244. (k) Perdew, J. P.; Chevary, J. A.; Vosko, S. H.; Jackson, K. A.; Pederson, M. R.; Singh, D. J.; Fiolhais, C. *Phys. Rev.* **1992**, *B46*, 6671.

ization on the homogeneous electron gas for correlation,[15c] augmented by gradient corrections to the exchange-correlation potential. Gradient corrections for exchange based on the functional of Becke[15d] and for the correlation based on Perdew[15e] were added variationally within the SCF procedure (LDA/BP-NLSCF).

All electron Gaussian orbital basis sets were used for all atoms. The calculations on the allyl and crotyl anion were performed with a standard TZVP basis which consists of a 10s/6p/1d set contracted to (7111/411/1) for carbon,[16b] and a 5s/1p set contracted to (311/1) for hydrogen.[16b] Concerning the (butenyl)(butadiene)(monoligand)nickel(II) complexes, the geometry optimization and the saddle-point search were done by using a standard DZVP basis which consists of a 15s/9p/5d set contracted to (63321/531/41) for nickel,[16a] a 18s/14p/9d set contracted to (633321/53321/531) for iodine,[16b] a 12s/8p/1d set contracted to (6321/521/1) for phosphorous,[16b] a 9s/5p/1d set contracted to (621/41/1) for carbon,[16b] and a 5s set contracted to (41) for hydrogen.[16b] This combination of basis sets will be referred to as basis-I. The energy was evaluated for the optimized structures using the Wachters 14s/9p/5d set[16c] supplemented by two diffuse p[16c] and one diffuse d function[16d] contracted to (62111111/5111111/3111) for nickel, and TZVP basen for iodine (the DZVP basis, where 2s and 2p contractions are decontracted and supplemented by a diffuse s and p function of about one-third of the most diffuse s and p function, respectively, thus yielding a (63331111/5331111/531) set) phosphorous[16b] (a 13s/9p/1d set contracted to (73111/6111/1)), carbon, and hydrogen, which will be denoted as basis-II. The corresponding auxiliary basis sets were used for fitting the charge density.[16b] This is the standard computational methodology used throughout this paper.

Concerning the [bis(allyl)-Ni-L] (L = PH_3, PMe_3) complexes, in addition to the LDA/BP-NLSCF treatment, optimizations were performed by using the gradient corrections for exchange based on the functional of Becke[15d] and the correlation functional of Lee, Yang, and Parr[15f,g] (BLYP-NLSCF). Moreover, calculations were carried out by utilizing the Gaussian-94[17] suite of programs with Becke's empirically parameterized three-parameter hybrid functional B3LYP.[15h] The B3LYP functional can be written as

$$F^{B3LYP} = (1 - A)F_xSlater + AF_xHF + BF_xBecke + CF_cLYP + (1 - C)F_cVWN$$

where F_xSlater is the Slater exchange,[15a,b] F_xHF is the Hartree-Fock exchange, F_xBecke is the gradient part of the exchange functional of Becke,[15d] F_cLYP is the correlation functional of Lee, Yang, and Parr,[15f,g] and F_cVWN is the correlation functional of Vosko, Wilk, and Nusair.[15c] The coefficients *A*, *B*, and *C* are determined by Becke using a fit to experimental heats of formation.[15h,i] It should be noted, however, that Becke did not use F_cVWN and F_cLYP in the expression above when the coefficients were determined, but rather the correlation functionals of Perdew and Wang.[15j,k]

The geometry optimization and the saddle-point search were carried out by utilizing analytical gradients/Hessians according to standard algorithms. No symmetry constraints were imposed in any case. The stationary points were exactly identified by the curvature of the potential-energy surface at these points corresponding to the eigenvalues of the analytically calculated Hessian. The zero-point energy corrections (ZPC) and Gibbs free energy calculations (at 298 K and 1 Atm) were performed for the reactants and products as well as the transition states for the rotational isomerism process. The electronic structure of the molecules is discussed using the natural bond orbital (NBO) population scheme.[18] Geometries of all of the relevant structures, which describe the isomerization in all of the complexes mentioned in this work, are given in the Supporting Information.

Results and Discussion

A. Allyl Anion and Crotyl Anion. The rotational automerism of the allyl anion as well as the rotational isomerism of 1-methylallyl (crotyl) anion has been the subject of extensive theoretical studies. The theoretically predicted equilibrium geometries and rotational barriers have already been reported.[19] Concerning the allyl anion, theoretically derived knowledge from those studies can be summarized as followed: The allyl anion has a planar geometry with C_{2v} symmetry. The important structural accommodation during the process of rotational automerism is the pyramidalization of the terminal carbon associated with sp^3 hybridization. There are two conformers of the transition state for the inward and outward rotation of the electron pair which is formed during the rotation (cf. Figure 2). According to Gobbi et al.[19a] the higher rotational barrier of the allyl anion relative to that of the allyl radical is essentially due to charge accumulation in the transition state. However, the covalent contributions of the delocalized π bonding to the rotational barriers have similar magnitude in both molecules. Additionally, concerning the allyl anion, they stated that the formation of the transition state is stabilized by hyperconjugation between the C−C π bond and the π orbital of the pyramidal methylene group. Therefore, the pyramidalization of the methylene group lowers the rotational barrier significantly.

The optimized structures of the allyl anion together with relative energies (ΔE) are depicted in Figure 3. Our results are in agreement with previously reported data.[19] The allyl anion has C_{2v} geometry with calculated C−C bond lengths of 140.0 pm. Most of the negative charge is localized at the terminal methylene groups (cf. Table 1). The transition state structures for rotational automerism, which are characterized by one short (C^1−C^2 ∼ 136 pm) and one long (C^2−C^3 ∼ 148 pm) C−C bond, have strong pyramidal methylene groups.[20]

(16) (a) DGauss basis set library. (b) Godbout, N.; Salahub, D. R.; Andzelm, J.; Wimmer, E. *Can. J. Chem.* **1992**, *70*, 560. (c) Wachters, A. H. J. *J. Chem. Phys.* **1970**, *52*, 1033. (d) Hay, P. J. *J. Chem. Phys.* **1977**, *66*, 4377.

(17) Frisch, M. J.; Trucks, G. W.; Schlegel, H. B.; Gill, P. M. W.; Johnson, B. G.; Robb, M. A.; Cheeseman, J. R.; Keith, T. A.; Petersson, G. A.; Montgomery, J. A.; Raghavachari, K.; Al-Laham, M. A.; Zakrzewski, V. G.; Ortiz, J. V.; Foresman, J. B.; Chioslowski, J.; Stefanov, B. B.; Nanayakkara, A.; Challacombe, M.; Peng, C. Y.; Ayala, P. Y.; Chen, W.; Wong, M. W.; Andres, J. L.; Replogle, E. S.; Gomperts, R.; Martin, R. L.; Fox, D. J.; Binkley, J. S.; Defrees, D. J.; Baker, J.; Stewart, J. P.; Head-Gordon, M.; Gonzalez, C.; Pople, J. A. *Gaussian 94*; Gaussian, Inc.: Pittsburgh, PA, 1995.

(18) Reed, A. E.; Curtiss, L. A.; Weinhold, F. *Chem. Rev.* **1988**, *88*, 899.

(19) (a) This is only a brief overview of the available theoretical studies. (b) Gobbi, A.; Frenking, G. *J. Am. Chem. Soc.* **1994**, *116*, 9275. (c) Foresman, J. B.; Wong, M. W.; Wiberg, K. B.; Frisch, M. J. *J. Am. Chem. Soc.* **1993**, *115*, 2220. (d) van Eikema Hommes, N. J. R.; Bühl, M.; Schleyer, P. v. R.; Wu, Y. D. *J. Organomet. Chem.* **1991**, *409*, 307. (e) Schleyer, P. v. R.; Kaneti, J.; Wu, Y. D.; Chandrasekhar, J. *J. Organomet. Chem.* **1992**, *426*, 143. (f) Chandrasekhar, J.; Andrade, J. G.; Schleyer, P. v. R. *J. Am. Chem. Soc.* **1981**, *103*, 5609. (g) Schleyer, P. v. R. *J. Am. Chem. Soc.* **1985**, *107*, 4793. (h) Wiberg, K. B.; Brenemann, C. M.; LePage, T. J. *J. Am. Chem. Soc.* **1990**, *112*, 61. (i) Wiberg, K. B.; Cheeseman, J. R.; Ochterski, J. W.; Frisch, M. J. *J. Am. Chem. Soc.* **1995**, *117*, 6535.

(20) The pyramidalization, given as the angle between C^2, C^3, and a dummy center located between the two hydrogens of the rotated methylene group, is $\angle$ C^2C^3D = 134.6° (127.8°) for TS-A (TS-B), respectively.

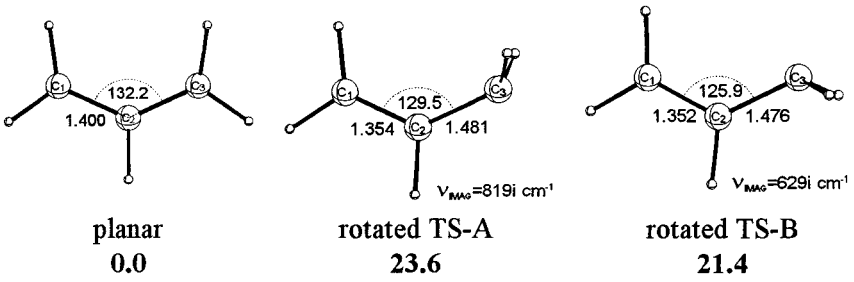

Figure 3. Selected geometric parameters of the optimized structures (Å, deg) for the rotational automerism of the allyl anion together with relative energies (ΔE in kcal/mol, TZVP+ basis).

Table 1. Charges in Allyl Anion[a]

	planar	TS-A[b]	TS-B[b]
C^1H_2	−0.458	−0.231	−0.203
C^2H_1	−0.084	−0.005	−0.046
C^3H_2	−0.458	−0.763	−0.751

[a] Based on natural population analysis, for atom labels see Figure 3. [b] For an explanation see the text.

In both transition states the C^1-C^2 bond is shorter with similar magnitude, while the C^2-C^3 bond is about 0.7 pm longer for the outward than for the inward rotation. Additionally, the $C^1C^2C^3$ bending angle is considerably decreased, combined with a stronger pyramidalization[20] of the rotated methylene group, in TS-B as compared with TS-A. The partial negative charge (cf. Table 1) at the rotated methylene group increases by 0.30 (0.29) electrons in TS-A (TS-B), respectively, relative to the planar form.

The automerization barrier via the energetically favored TS-B and the alternative TS-A is 24.4 and 26.7 kcal/mol, respectively (TZVP basis). It decreases by about 3.0 kcal/mol if diffuse functions on all atoms are included[21a] (TZVP+ basis), thus giving a rotational barrier of 21.4 and 23.6 kcal/mol via inward and outward rotation, respectively. The ZPC and corrections arising from thermal motion influence the barrier by a nearly identical, but opposite amount. Thus the potential energy profile (ΔE) is not substantially affected by them. The energetic preference of the inward versus the outward rotation is in accord with previous theoretical studies.[19] Concerning the lowest energy barrier, Gobbi et al.[19a] reported a value of 23.1 kcal/mol [MP2/6-31G-(d)//HF/6-31G], Schleyer et al.[19c] reported a value of 21.7 kcal/mol [MP2/6-31G+(d,p)], and Wiberg et al. gives values of 20.9 kcal/mol[19b] [MP2-FU/6-31G+(d)] and of 20.3 kcal/mol[19h] at the G2 level of computation.

The optimized structures of the crotyl anion together with relative energies (ΔE) are given in Figure 4. Due to the methyl substitution there are two isomers, anti and syn,[8] of the planar crotyl anion. In accordance to Schleyer et al.[19d] the same conformation of the methyl group with regard to the adjacent hydrogen was found as the most stable planar anti and syn forms.

The delocalized π bonds are nearly identical in both planar forms and the optimized bond lengths are quite comparable to the allyl anion. A similar distribution of the negative charge as in the allyl anion can be discerned from Table 2. The anti isomer is found to be 3.0 kcal/mol more stable than the syn form (TZVP+ basis). The most reliable energy difference reported by Schleyer et al.[19d] is 4.6 kcal/mol [MP2/6-31G+//3-21G].

Both conformers of the rotational transition structures are now chiral due to the methyl substitution.

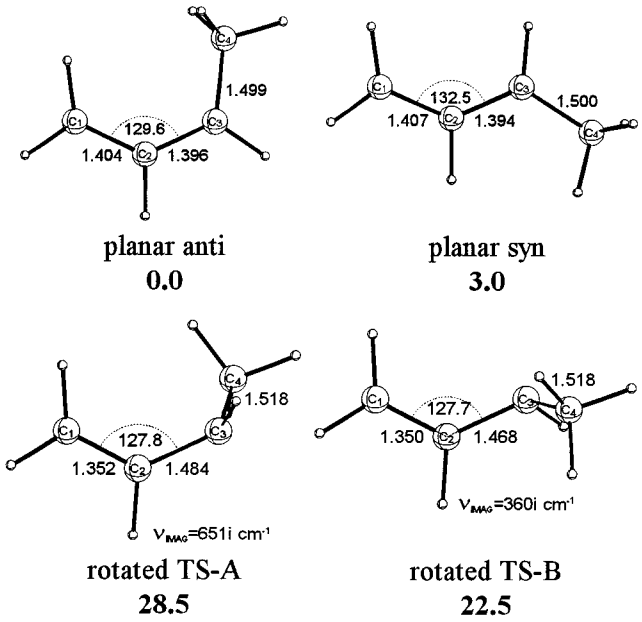

Figure 4. Selected geometric parameters of the optimized structures (Å, deg) for the rotational isomerism of the crotyl anion together with relative energies (ΔE in kcal/mol, TZVP+ basis).

Table 2. Charges in Crotyl Anion[a]

	planar-anti	planar-syn	TS-A[b]	TS-B[b]
C^1H_2	−0.463	−0.456	−0.206	−0.182
C^2H_1	−0.085	−0.093	−0.007	−0.059
C^3H_1	−0.329	−0.326	−0.624	−0.593
C^4H_3	−0.123	−0.124	−0.162	−0.166

[a] Based on natural population analysis, for atom labels see Figure 4. [b] For an explanation see the text.

Therefore, two enantiomorph forms exist for each of the conformers TS-A and TS-B. The distortion of the allylic moiety follows the same trends discussed for the allyl anion. An important feature of the rotational isomerism is the lengthening of the C^3-C^4 bond by a very similar magnitude of about 1.8 pm in both conformers (cf. Figure 4).

In agreement with the similar distortion of the allylic part, the changes in the charge distribution are also quite comparable to the allyl anion (cf. Table 2). Upon rotation the negative charge of the methyl substituted methylene group has increased by 0.30 (0.27) electrons in TS-A (TS-B), respectively, with a slightly increased negative charge on the methyl group.

The rotational isomerism in the crotyl anion preferably take place via inward rotation toward TS-B. The barrier amounts to 27.0 (24.5) kcal/mol relative to the planar anti (syn) anion, respectively (TZVP basis), which

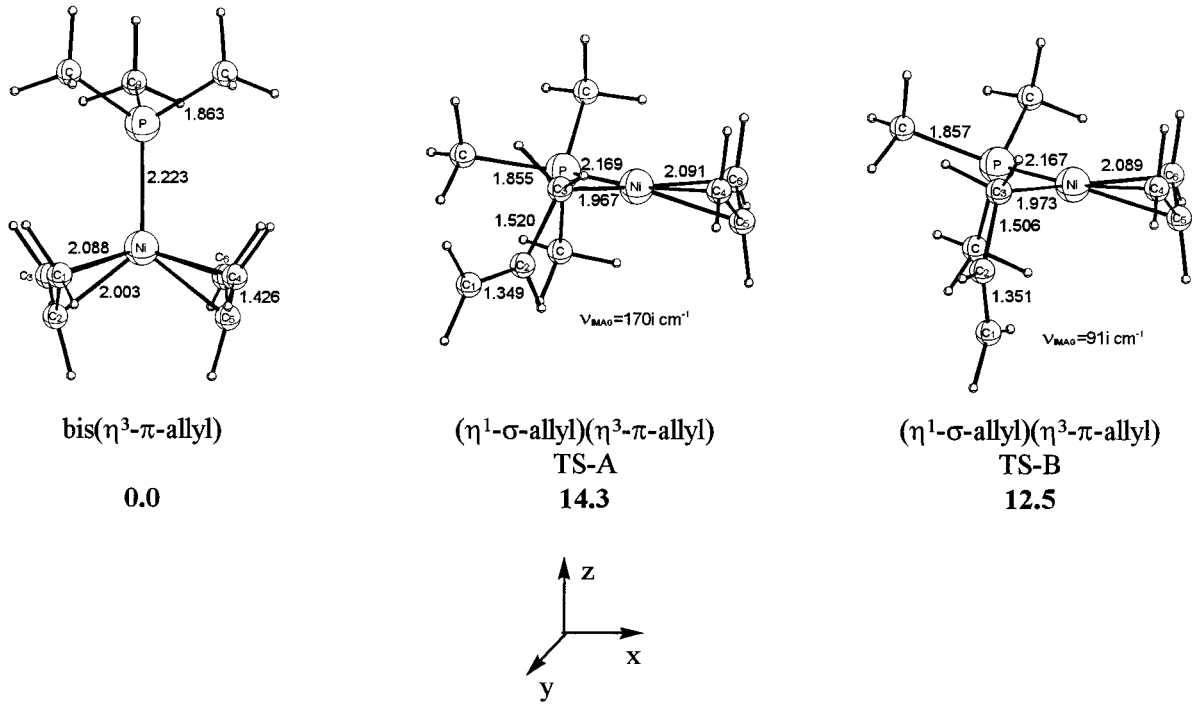

Figure 5. Selected geometric parameters of the optimized structures (Å) for the rotational automerism of one allyl group in [bis(allyl)-Ni-PMe_3] together with relative energies (ΔE in kcal/mol, LDA/BP(basis-I)).

is decreased to 22.5 and 19.5 kcal/mol, respectively, if the TZVP+ basis is employed. Similar to the allyl anion the barriers are not remarkably influenced if both ZPC and entropy corrections are included. The outward rotation is 6.0 kcal/mol less favored than the inward rotation.

The geometric structure and the charge distribution for the planar and rotated forms of the allyl and crotyl anions, which are not noticeably affected by the methyl group, are calculated in close agreement with previous theoretical studies.[19] Commencing from the most stable planar isomer, the barrier along the favored inward rotation is 1.1 kcal/mol higher for the crotyl anion than for the allyl anion. As α-alkyl substituents generally destabilize carbanions,[19c,19d,21] they also must, perhaps to a greater extent, destabilize the rotated forms.

B. [Bis(allyl)-Ni-L] (L = PH_3, PMe_3) Complexes. The [bis(η^3-allyl)-M] complexes of the nickel triad, where M = Ni, Pd, Pt, may react with donor ligands by addition followed by rearrangement or displacement of one or both η^3-π-allyl groups. From their NMR measurements Wilke et al.[22] estimated the automerization barrier of one allyl group in the [bis(η^3-allyl)-Ni-PMe_3] complex as the free energy of activation ($\Delta G^{\#}$) to 9.6 ± 1.5 kcal/mol.

We begin by examining the effect of the basis set and DFT Hamiltonian on the geometric parameters of the [bis(η^3-allyl)-Ni-L] complexes. Then we discuss their influence on the calculated automerization barrier. Apart from our standard methodology, full geometric optimization is performed at the LDA/BP, BLYP and B3LYP levels of computation utilizing both basis-I and basis-II. PH_3 is adopted as a much less computationally demanding model of the real PMe_3 ligand. The skeletal geometry optimized for the bis(η^3-allyl) complexes and the rotational transition structures are very similar for both donor ligands. Therefore, the optimized structures of only the PMe_3 complexes are displayed in Figure 5.

First, we start with the [bis(η^3-allyl)-Ni-L] complexes. In accordance with the X-ray structural data of the PMe_3 complex[22] the minimum energy structures calculated are characterized by a supine−supine orientation of both allylic moieties. The 18-electron tetragonal pyramidal coordinated complexes possess approximately C_s symmetry, the mirror plane passing through the atoms Ni, P, and C_9 (cf. Figure 5). Additionally, a partial C_s symmetry can be detected within the bis(η^3-allyl)-Ni fragment, where the mirror plane is defined by the centers of both terminal allylic carbons and the Ni atom. Therefore, while focusing on the most important geometric degrees of freedom, only the average geometric parameters are discussed with reference to the assumed symmetry planes.

In addition to the data given in Figure 5, selected geometric parameters are collected in Table 3 for [bis(allyl)-Ni-PMe_3] along with experimental data and for [bis(allyl)-Ni-PH_3] in Table 4. For the PMe_3 complex, the geometric parameters are calculated in excellent agreement with the X-ray data, even if the smaller basis is employed. The skeletal geometry is calculated to be very similar for both complexes, except for the Ni−ligand bond that is slightly shorter for PH_3 than for PMe_3. Both the LDA/BP and the B3LYP levels provide reasonably similar results by using both basis sets, with the LDA/BP level seems to be slightly superior. On the other hand, the Ni−carbon bond length predictions are too long when the BLYP approximation is used. If the

(21) (a) Clark, T.; Chandrasekhar, J.; Spitznagel, G. W.; Schleyer, P. v. R. *J. Comput. Chem.* **1984**, *4*, 294. (b) Spitznagel, G. W.; Clark, T.; Chandrasekhar, J.; Schleyer, P. v. R. *J. Comput. Chem.* **1982**, *3*, 363. (c) Schleyer, P. v. R.; Spitznagel, G. W.; Chandrasekhar, J. *Tetrahedron Lett.* **1986**, *27*, 4411.

(22) Henc, B.; Jolly, P. W.; Salz, R.; Stobbe, S.; Wilke, G.; Benn, R.; Mynott, R.; Seevogel, K.; Goddard, R.; Krüger, C. *J. Organomet. Chem.* **1980**, *191*, 449.

Table 3. [Bis(η^3-π-allyl)-Ni-PMe_3]: Selected Geometric Parameters[a]

	LDA/BP basis-I/(II)	B3LYP basis-I/(II)	expt[b]
Ni-C^1	208.3(209.5)	209.2(210.7)	207.4
Ni-C^2	200.3(200.5)	201.3(202.3)	199.4
C^1-C^2	142.6(142.0)	141.7(140.9)	141.0
C^1-C^2-C^3	118.1(118.5)	119.0(119.4)	118.5
Ni-P	222.3(223.5)	227.1(229.3)	221.7
P-C	186.3(186.2)	185.6(185.6)	183.7
C-P-C	100.5(100.4)	100.5(100.5)	101.1

[a] Averaged geometric parameters, as described in text. Distances in angstroms, angles in deg, values in parenthesis refer to basis-II. For atom labels see Figure 5. [b] Averaged geometric parameters from ref 21.

Table 4. [Bis(η^3-π-allyl)-Ni-PH_3]: Selected Geometric Parameters[a]

	LDA/BP basis-I/(II)	BLYP basis-I/(II)	B3LYP basis-I/(II)
Ni-C^1	208.6(209.7)	212.8(213.5)	209.3(211.0)
Ni-C^2	200.3(200.4)	203.8(203.7)	201.1(202.2)
C^1-C^2	142.5(141.9)	142.6(141.9)	141.6(140.8)
C^1-C^2-C^3	118.5(119.0)	119.5(119.7)	119.3(119.8)
Ni-P	221.8(221.7)	226.2(226.0)	225.9(227.8)
H-P-H	95.5(94.7)	95.5(95.1)	95.2(95.4)

[a]Averaged geometric parameters, as described in text. Distances in angstroms, angles in deg, values in parentheses refer to basis-II. For atom labels see Figure 5.

Table 5. Charges in [Bis(allyl)-Ni-L] for L = PMe_3 and PH_3 (in Italics)[a]

		(η^1-σ-allyl)(η^3-π-allyl)	
	bis(η^3-π-allyl)	TS-A[b]	TS-B[b]
C^1H_2	−0.169/*−0.161*	−0.038/*−0.034*	−0.074/*−0.061*
C^2H_1	−0.081/*−0.078*	−0.023/*−0.015*	0.006/*0.003*
C^3H_2	−0.173/*−0.162*	−0.383/*−0.385*	−0.376/*−0.377*
Σ_{allyl}	−0.423/*−0.401*	−0.444/*−0.434*	−0.444/*−0.435*
C^4H_2	−0.169/*−0.161*	−0.152/*−0.146*	−0.140/*−0.139*
C^5H_1	−0.081/*−0.078*	−0.039/*−0.041*	−0.036/*−0.037*
C^6H_2	−0.173/*−0.162*	−0.200/*−0.166*	−0.202/*−0.168*
Σ_{allyl}	−0.423/*−0.401*	−0.391/*−0.353*	−0.378/*−0.344*
Σ_{ligand}	0.138/*0.093*	0.277/*0.217*	0.272/*0.215*
Ni	0.708/*0.709*	0.559/*0.571*	0.550/*0.565*

[a] Based on natural population analysis at LDA/BP(basis-I) level; for atom labels see Figure 5. [b] For an explanation see the text.

larger basis-II is employed, no substantial changes in the important geometric degrees of freedom are obvious.

The allylic moieties carry a large negative charge, which is mainly localized at the terminal methylene groups (cf. Table 5). As expected, PMe_3 is the stronger donor which, therefore, gives rise to an enhanced magnitude of the allylic part's negative charge.

During the process of rotational automerism, which is accompanied by a $\pi \rightarrow \sigma$ conversion of one allyl group while retaining the other allyl group in π-coordination to nickel, the coordination sphere around the transition metal changes from tetragonal pyramidal (18-electron [bis(η^3-allyl)-Ni-L]) to square-planar (16-electron [η^1/η^3-allyl-Ni-L]). Similar to the free allyl anion case, there are two rotational transition isomers. The LDA/BP and B3LYP level predict very similar geometry, which is not noticeably affected by employing basis-II. The largest deviation from that observed at BLYP level occurred at the Ni−C^1 distance, which is elongated by 1.5 pm.[23] Thus the LDA/BP level employing basis-I can be regarded as suitable to reliable when predicting the geometry of both of the π-allyl and σ-allyl forms. The B3LYP level is also able to reproduce the geometric structure with great accuracy, but the geometric parameters will only be discussed at the LDA/BP level of calculation.

(23) See the structural data given in the Supporting Information.

Table 6. Calculated Potential-Energy (with and without ZPC) and Gibbs Free Energy Profile for the Rotational Automerization in [Bis(allyl)-Ni-L] Complexes (L = PH_3, PMe_3) (kcal/mol)[a]

		(η^1-σ-allyl)(η^3-π-allyl)	
	bis(η^3-π-allyl)	TS-A[b]	TS-B[b]
L = PH_3			
LDA/BP basis-I	0.0 (0.0)	17.2 (16.3)	14.6 (14.1)
	0.0	*14.9*	*13.6*
LDA/BP basis-II[c]	0.0	16.5	14.2
	0.0	*14.2*	*13.2*
BLYP basis-I	0.0 (0.0)	12.0 (11.6)	9.8 (9.5)
	0.0	*10.7*	*9.3*
BLYP basis-II[c]	0.0	10.9	9.6
	0.0	*9.6*	*9.1*
B3LYP basis-I	0.0	11.4	9.1
B3LYP basis-II	0.0	10.0	7.8
L = PMe_3			
LDA/BP basis-I	0.0 (0.0)	14.3 (13.8)	12.5 (12.3)
	0.0	*12.3*	*11.5*
LDA/BP basis-II[c]	0.0	13.4	11.4
	0.0	*11.4*	*10.4*
B3LYP basis-I	0.0	8.2	6.2
B3LYP basis-II	0.0	6.9	5.1

[a] Numbers in parentheses include the zero point corrections, while those in italics are the Gibbs free energies. [b] For an explanation see the text. [c] Concerning basis-II the Gibbs free energies are estimated based on the corresponding results of the frequency calculation obtained with basis-I.

Similar to the findings for the [bis(η^3-allyl)-Ni-L] complexes concerning the rotational transition structures, the influence of the different donating ability of both PH_3 and PMe_3 ligands cannot be clearly observed from the allylic group's geometry. However, the Ni−ligand bond is about 2.2 pm longer for PMe_3 than for PH_3.[23]

The changes in geometry of the allylic moiety, which undergoes the η^3-$\pi \rightarrow \eta^1$-σ rearrangement, is similar to the changes observed for the free allyl anion (cf. Figure 5). The C^1−C^2 bond is shortened with similar magnitude in both transition structures; and the C^2−C^3 is about 1.3 pm longer for TS-A than for TS-B.

The changes in the charge distribution that occurred in the converted allylic moiety are fairly unaffected whether the PH_3 or PMe_3 ligands are concerned and are similar to those found in the allyl anion (cf. Table 5). The partial negative charge at the rotated methylene group has increased by about 0.21 (0.20) electrons in TS-A (TS-B), respectively, relative to the bis(π-allyl) form. Overall, during the internal rotation process, a small amount of negative charge (approximately 0.02 electrons) is accumulated at the entire $\pi \rightarrow \sigma$ converted allylic part, whereas the negative charge decreases to a similar amount in the retained π-allylic part and to a larger amount (about 0.13 electrons) for the ligand.

In Table 6 the rotational barriers calculated at different computational levels and basis sets employed are summarized. Their influence on the activation energy is examined for the potential energy (ΔE). In accordance with the allyl anion, in each case the calculations predict the rotational automerization pref-

erably takes place via the inward transition state conformer (i.e., TS-B). First the PH_3 complex is considered, followed by the PMe_3 complex.

The activation energy necessary to overcome TS-B is 14.6 kcal/mol at the LDA/BP(basis-I) level. This is about 5.0 kcal/mol higher than the predicted activation energy at the BLYP and B3LYP levels, which are 9.8 and 9.1 kcal/mol, respectively. The corresponding outward transition state (TS-A) is about 2.5 kcal/mol higher, irrespective of which computational level is utilized. The automerization barrier decreases slightly by applying basis-II and with the inclusion of ZPC and entropic effects. The PH_3 model system seems to be an inappropriate model to judge the reliability of the computational approach to satisfactorily predict the experimentally determined automerization barrier of the [bis(allyl)-Ni-PMe_3] complex, because of the well-known different electronic and steric properties of both ligands.

For the PMe_3 complex, TS-B is calculated to be 12.5 kcal/mol above the bis(η^3-allyl) complex at the LDA/BP-(basis-I) level. The barrier is lowered to 11.4 kcal/mol (ΔE) and 10.4 kcal/mol (ΔG) by applying basis-II, which agrees very well with the experimental value of 9.6 ± 1.5 kcal/mol[22] (derived as $\Delta G^{\#}$). The inclusion of additional diffuse functions[21a] on carbon and hydrogen has a minor influence on the activation energy, at the most, 0.3 kcal/mol. For the σ-C^3 intermediates (cf. Figure 2) the energy needed for the internal rotation around the Ni−C^3 σ-bond is estimated to be about 2.1 kcal/mol lower than that required around the C^2−C^3 σ-bond (via TS-B). The rotational barrier across TS-B decreases by about 2.8 kcal/mol when replacing PH_3 with PMe_3 (LDA/BP(basis-II)), which is analyzed according to reaction 1.

$$[\text{Ni-}(\eta^3/\eta^1\text{-}C_3H_5)(\eta^3\text{-}C_3H_5)\text{-L}] + \text{L}' \rightarrow [\text{Ni-}(\eta^3/\eta^1\text{-}C_3H_5)(\eta^3\text{-}C_3H_5)\text{-L}'] + \text{L} \quad (1)$$

where L = PH_3, L′ = PMe_3

The stronger donor, PMe_3, stabilizes the σ-allyl rotational transition structure by 17.3 kcal/mol and the bis-(π-allyl) form by 14.5 kcal/mol (LDA/BP(basis-II)), which therefore gives rise to a reduced barrier upon ligand exchange.

The automerization barrier is predicted to be 6.2 kcal/mol at the B3LYP(basis-I) level. It is 5.1 kcal/mol by applying basis-II and should be further decreased if ZPC and entropy contributions are included. Compared with the experimental value it is clear that the rotational barrier is underestimated at the B3LYP level of computation. Therefore, although both LDA/BP and B3LYP levels are good choices to predict the geometric parameters to a highly accurate degree, only the LDA/BP level can be deemed satisfactory in predicting the automerization barrier. The results presented in this section suggest that the standard computational methodology allows one to investigate the butenyl group isomerization, discussed in subsequent sections, with a high degree of confidence.

C. Cationic [Ni(allyl)(butadiene)L]$^+$ (L = PF_3, PH_3, PMe_3, C_2H_4) and Neutral [Ni(allyl)(butadiene)I] Complexes. The complexes investigated in this section are labeled as follows: [Ni(C_3H_5)(C_4H_6)L]$^+$, **I**, and [Ni(C_3H_5)(C_4H_6)I], **III**, with the neutral ligands identified by an additional lower case letter; i.e., **a**, **b**, **c**, and **d** for PF_3, PH_3, PMe_3, and C_2H_4, respectively. The optimized geometry of η^3-π-allyl complexes and of relevant rotational transition η^1-σ-allyl structures together with relative energies (ΔE) are displayed in Figure 6 for **Ib**, **Id**, and **III**. The calculated geometries are hardly influenced by different PR_3 ligands, regardless of whether π-allyl or σ-allyl forms are concerned. Therefore, for PR_3 ligands, the discussion of the geometric parameters focuses on PH_3.

1. η^3-π-Allyl Complexes. We have already investigated[7a] the stability of 18-electron (η^3-π-butenyl)(η^4-butadiene)(monoligand)Ni(II) complexes. The most stable orientation arises from a tetragonal pyramidal coordination with a supine−supine[11] arrangement of both η^3-allyl and η^4-butadiene moieties and the axial position occupied by the ligand.

The bonding, as explained in terms of the main orbital interactions (cf. Figure 7), can be attributed to an interaction of the HOMO's of both the allylic (nonbonding 2π) and the butadiene (2π) moieties with the formal vacant Ni d_{xy} orbital (Figure 7a). The ligand, which occupies the axial position above the quasi planar coordination plane, may interact with the metal through σ-donation from occupied orbitals (i.e., the lone pair for PR_3, iodine anion, and ethylene's π-orbital) into corresponding empty metal orbitals (i.e., Ni 4s) (Figure 7b) and via π-back-donation from occupied metal orbitals (i.e., Ni d_{xz}, d_{yz}) into vacant ligand orbitals of appropriate symmetry (Figure 7c and d). In the case of PR_3 ligands and the iodine anion, no clear indication for participation of the ligand's acceptor orbitals in the overall bonding interaction can be observed. The nickel−ligand bonding will be attenuated by the repulsive interaction of the ligand's σ-orbitals, which are directed toward the metal, with the Ni d_{zz} (Figure 7e). The ligand donation enlarges the electron density on the metal, thus decreasing the acceptor strength of the metal, which gives rise to a redistribution toward the allylic and butadiene parts. This is accomplished through a Ni σ-back-donation toward allyl ($d_{xz} \rightarrow 3\pi^*$) and toward butadiene ($d_{zz}$ (d_{xz}) $\rightarrow 3\pi^*$), with the latter being preferred (Figure 7f). Thus, the larger the ligand acting as a donor, the more efficiently the repulsive interaction with Ni d_{zz} can be avoided, which in addition contributes to amplifying the Ni ligand bond.

Overall, the η^3-allyl complexes almost approach C_s symmetry, except for the ethylene ligand, which is diagonal coordinated between the *xz* and *yz* planes, and therefore gives rise to an unsymmetrical coordination of the allyl and butadiene moieties (cf. Figure 6). The allylic part is distorted to a very similar extent for each of the ligands investigated. The C−C bonds are elongated by about 1.5 pm and the $C^1C^2C^3$ bending angle is decreased by about 18°, relative to the free allyl anion.[23] Obviously, neither of the ligand's donor strength can compete with that of the allyl anion, which would give rise to a significant Ni to allyl back-donation, which we consider responsible for allylic distortion due to the ligand's influence. On the other hand, the ligand's influence clearly can be discerned from butadiene. The C^5−C^6 bond is shortened with increasing ligand donating ability, by about 1.6 pm in **Ia** and by about 2.5 pm

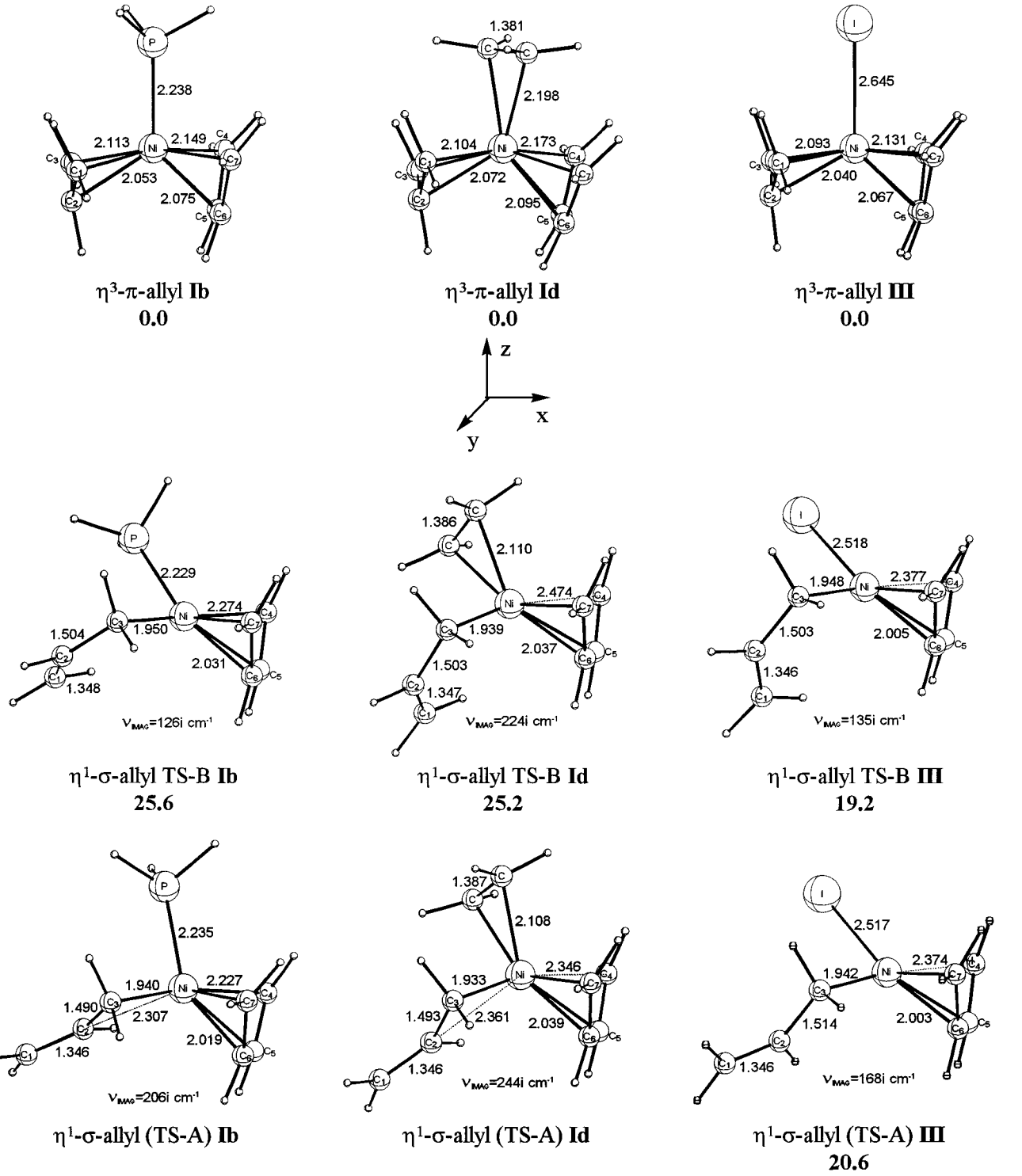

Figure 6. Selected geometric parameters of the optimized structures (Å) for the rotational automerism of the allyl group in [Ni(allyl)(butadiene)-L/I]$^{(+)}$ complexes together with relative energies (ΔE in kcal/mol).

in **Ic**.[23] Additionally, the terminal $C^4{=}C^5$ and $C^6{=}C^7$ double bonds are elongated by approximately 1.7 and 2.3 pm concerning PF_3 and PMe_3, respectively.[23] We consider the Ni to butadiene back-donation ($d_{zz} \rightarrow 3\pi^*$) mainly responsible for both effects.

From Table 7 it is clear that the donor strength of the PR_3 ligands increases in the order $PF_3 < PH_3 < PMe_3$. As expected, the iodine anion is the strongest donor. Both for the PR_3 ligands and the iodine anion there are no indications that empty acceptor orbitals participate in the bonding interaction. On the other hand, the small partial charge of ethylene points to a well-balanced donor and acceptor ability in this case. Overall, the amount of negative charge accumulated in the allylic and butadiene parts goes along with the ligand's donor strength, where butadiene is the much better acceptor, similar to the geometric distortion observed.

The influence of the ligand on the overall stability is evaluated by means of reaction 2 (cf. Table 8), where

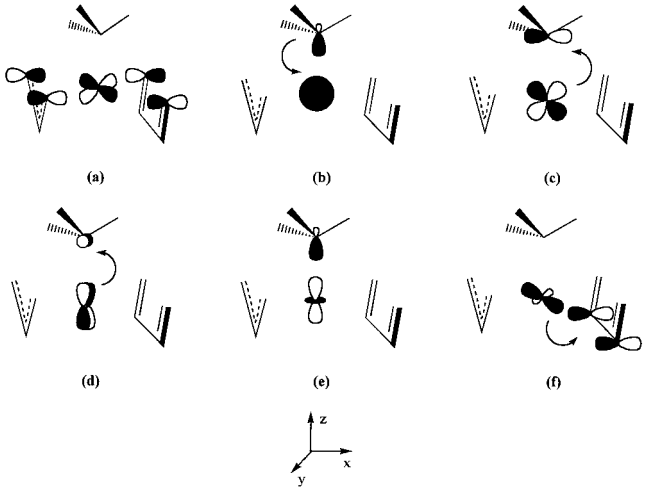

Figure 7. Important orbital interactions in [Ni(π-butenyl)-(butadiene)-L/I]$^{(+)}$ complexes, schematic sketched concerning L = PR_3.

PH_3 was chosen as the reference.

$$[(\eta^3\text{-}\pi\text{-}C_3H_5)(\eta^4\text{-}C_4H_6)Ni\text{-}PH_3]^+ + L/I \rightarrow [(\eta^3\text{-}\pi\text{-}C_3H_5)(\eta^4\text{-}C_4H_6)Ni\text{-}L/I]^{(+)} + PH_3 \quad (2)$$

Consistent with the observed charge transfer, the strong donors PMe_3 and the iodine anion yield the largest overall stabilization. For **III** the stabilization is further enlarged by a considerable amount, due to the electrostatic interaction between cation and anion. Concerning the weaker donor ligands, PF_3 and ethylene, a destabilization relative to PH_3 appears, which is estimated at 9.5 kcal/mol (**Ia**) and 10.0 kcal/mol (**Id**), respectively.

2. η^1-σ-Allyl Complexes. As discussed for the [bis-(allyl)-Ni-L] complexes, the rotational transition structures are characterized by an empty coordination site on the nickel center. Both isomers for the outward (TS-A) and inward (TS-B) rotation were determined. However, due to the strong acceptor strength of the Ni(II) center in the coordinatively unsaturated cationic complexes, the metal tends to form an additional bond to the rotated allyl group. Thus, for **I** the allylic part preferably is η^2-coordinated in TS-A. This hindered internal rotation around C^2-C^3 is prevented in TS-B, since the C^2-carbon is turned back from the nickel center. With a strong donor, i.e., the iodine anion, in both isomers of **III** no hindrance occurs (cf. Figure 6). For the cationic complexes **I**, TS-A cannot be regarded as the transition states for the free rotation around C^2-C^3 that were passed along the minimum energy pathway. Therefore, only TS-B will be considered for **I**.

The σ-allyl rotational transition states have quasi square-planar structures that are slightly distorted since the ligand is moved to a certain degree away from the planar coordination plane (cf. Figure 6) in order to avoid the repulsive interaction with the cis σ-allyl group. Simultaneously, the coordination of the butadiene double bond $C^4{=}C^5$, trans to the allyl group, to Ni(II) is weakened, as indicated by the corresponding elongated Ni−C bonds displayed in Figure 6.

The bonding in TS-B can be mainly attributed to the interaction of the HOMO's of the rotated allyl group (free electron pair), of butadiene (2π) and of the ligand (spσ lone pair for PR_3 and the iodine anion, and π for ethylene) with the formal vacant Ni d_{xy} orbital (cf. Figure 8). Apart from the Ni(d) → ethylene(π*) back-donation, the analysis of the important orbital interactions gives no indication of any other back-donation contribution of the metal with the allylic, butadiene, or ligand parts. Therefore, the calculations reveal that the butadiene changes its donor−acceptor characteristic upon the automerization process. For the π-allyl reactants its acceptor property predominates, whereas for the σ-allyl transition structures butadiene essentially acts as a donor (cf. Table 7).

Similar to the η^3-π-allyl complexes, the geometry of the η^1-σ-allyl group is not noticeably influenced by the different ligands. The changes in the allylic group's geometry during the $\pi \rightarrow \sigma$ conversion are comparable to those found in the free allyl anion. The C^2-C^3 bond is elongated to nearly the same amount (about 9 pm), whereas the vinyl C^1-C^2 bond is shortened by about 7 pm, compared with the 4.7 pm for the free allyl anion.[23]

The rotational automerization preferably takes place through inward rotation of the free electron pair toward TS-B for all ligands considered (cf. Table 9). For **III** the competitive outward rotation via TS-A lies 1.4 kcal/mol (ΔE) above. The free energy rotational barrier decreases in the following order; PF_3 (28.4 kcal/mol) > PH_3 (23.4 kcal/mol) > PMe_3 (21.4 kcal/mol) > I^- (16.7 kcal/mol), while the ligand's donor strength increases.

Similar to reaction 2 the overall stability of TS-B influenced by the ligand is evaluated by reaction 3 (cf. Table 8).

$$[(\eta^1\text{-}\sigma\text{-}C_3H_5)(\eta^4\text{-}C_4H_6)Ni\text{-}PH_3]^+ \text{(TS-B)} + L/I \rightarrow [(\eta^1\text{-}\sigma\text{-}C_3H_5)(\eta^4\text{-}C_4H_6)Ni\text{-}L/I]^{(+)} \text{(TS-B)} + PH_3 \quad (3)$$

When PH_3 is considered as an arbitrary reference, stronger donors such as PMe_3 and the iodine anion stabilize the rotational transition form, whereas the less basic PF_3 destabilizes it. With respect to the relative stabilities of the corresponding π-allyl complexes, PMe_3 and the iodine anion favor the σ-allyl structure, thus lowering the barrier by 2.3 and 6.4 kcal/mol, respectively, relative to PH_3. On the other hand, for PF_3 the allylic group rotation is defavored by 4.6 kcal/mol, relative to PH_3. The activation free energy of automerization for **Ic** is almost identical to that for the free allyl anion (cf. Figure 3), which is 4.7 kcal/mol higher than the activation free energy for **III**.

For donor ligands, i.e., PR_3 and I^-, the automerization barrier is essentially determined by their donating ability. The activation energy decreases with increasing ligand donor strength, due to a pronounced stabilization of the σ-allyl rotational transition state by strong donors. The stability of the σ-allyl structure is correlated with the entire allylic part's formal negative charge (cf. Table 7), which is mainly located at the rotated C^3H_2 methylene group. However, the amount of accumulated negative charge in the allylic part upon $\pi \rightarrow \sigma$ conversion is nearly identical (0.14 electrons) for PR_3 ligands. This can be understood if one is aware of the π-acidity of butadiene, which may be responsible for a negative charge migration toward allyl, but only to a certain degree. Since there is already a marked transfer of

Table 7. Charges in Cationic [Ni(allyl)(butadiene)L]$^+$ (I) and Neutral [Ni(allyl)(butadiene)I] (III)[a]

	C^1H_2	C^2H	C^3H_2	Σ_{allyl}	$\Sigma_{butadiene}$	L/I	Ni
η^3-π-allyl							
Ia (L = PF_3)	0.039	−0.016	0.036	0.059	0.041	0.259	0.642
Ib (L = PH_3)	0.008	−0.021	0.009	−0.004	−0.031	0.285	0.751
Ic (L = PMe_3)	−0.007	−0.021	−0.013	−0.041	−0.088	0.368	0.760
Id (L = C_2H_4)	0.045	−0.018	0.028	0.056	0.070	0.012	0.863
III	−0.016	−0.068	−0.016	−0.100	−0.164	−0.537	0.800
η^1-σ-allyl TS-B[b]							
Ia (L = PF_3)	0.011	0.018	−0.116	−0.088	0.132	0.326	0.630
Ib (L = PH_3)	−0.001	0.017	−0.160	−0.145	0.088	0.352	0.704
Ic (L = PMe_3)	−0.012	0.013	−0.184	−0.182	0.057	0.442	0.683
Id (L = C_2H_4)	0.012	0.011	−0.079	−0.055	0.126	0.057	0.873
III	−0.025	0.004	−0.190	−0.211	−0.085	−0.438	0.734

[a] Based on natural population analysis; for atom labels, see Figure 6. [b] For an explanation see the text.

Table 8. Calculated Changes in Total Energy (ΔE in kcal/mol) for the Relationships in Equations 2−5

L/I	η^3-π-allyl eq 2	η^1-σ-allyl TS-B eq 3	η^3-π-crotyl eq 4	η^1-σ-crotyl TS-B eq 5
PF_3	9.5	14.1	−6.6	1.1
PH_3	0.0	0.0	−5.6	2.1
PMe_3	−12.2	−14.5	−4.9	5.3
C_2H_4	10.0	9.5	−6.0	0.9
I	−89.2	−95.6	−3.8	3.2

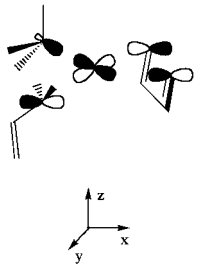

Figure 8. Important orbital interactions in [Ni(σ-butenyl)-(butadiene)-L/I]$^{(+)}$ complexes, schematic sketched concerning L = PR_3.

electron density in the π-allyl complex of **III**, automerization then requires only 0.11 electrons to migrate.

The net donor strength of ethylene and PF_3 is of similar magnitude (cf. Table 7). This agrees with the calculated relative stability of the π-allyl complexes. However, in contrast to **Ia**, ethylene supports the formation of the σ-allyl structure, which in turn gives rise to an activation barrier between the barriers of **Ia** and **Ic**. This can be attributed to the π-acidity of ethylene. The back-donation into the π*-orbital on ethylene increases during the allyl group's conversion, as indicated by the elongation of the olefinic double bond (cf. Figure 6). Therefore, as opposed to the case of donor ligands, when regarding ethylene, we consider its π-acidity responsible for stabilizing the σ-allyl form.

D. Cationic [Ni(crotyl)(butadiene)L]$^+$ (L = PF_3, PH_3, PMe_3, C_2H_4) and Neutral [Ni(crotyl)(butadiene)I] Complexes. The complexes examined in this section are denoted as follows: [Ni(C_4H_7)(C_4H_6)L]$^+$, **II**, and [Ni(C_4H_7)(C_4H_6)I], **IV**, with the neutral ligands labeled in the same manner as in section C. The calculated geometries and the bonding interaction of both of the η^3-π- and the η^1-σ-crotyl forms of (crotyl)-(butadiene)(monoligand)Ni(II) complexes resemble those of the corresponding allyl complexes. The only exception concerns the crotyl π-coordination, which is now, due to the methyl group, unsymmetrical with the Ni−C^3 distance being longer than the Ni−C^1 distance. The investigation will therefore be focused on the energetics and the changes in the butenyl part's charge distribution due to the methyl substitution.

1. η^3-π-Crotyl Complexes. In Figure 9 the displayed optimized geometry of both of the anti and syn forms of the η^3-π-crotyl complex and of TS-B is restricted to **IIb**. Overall, for the π-crotyl complexes the syn form is more stable than the anti form (cf. Table 9). That differs from the case for the free crotyl anion and can be attributed to an enhanced unfavorable steric interaction of the axial ligand with the butenyl group in the anti relative to the syn form. The energy difference (ΔE) between the two forms is about 3.0 kcal/mol, except for **IIc** which is 4.6 kcal/mol for the sterically most demanding PMe_3 ligand of our research. To study the influence of the methyl group upon the stability of the π-butenyl form, reaction 4 is considered (cf. Table 8):

$$[(\eta^3\text{-}\pi\text{-}C_3H_5)(\eta^4\text{-}C_4H_6)\text{Ni-L/I}]^{(+)} + \text{planar } [syn\text{-}C_4H_7]^- \rightarrow [(\eta^3\text{-}\pi\ syn\text{-}C_4H_7)(\eta^4\text{-}C_4H_6)\text{Ni-L/I}]^{(+)} + \text{planar } [C_3H_5]^- \quad (4)$$

Overall, an enhanced stability results when replacing allyl with crotyl. Thus a methyl substitution will amplify the π-coordination of the butenyl group. The stabilization due to the methyl group is found to be more pronounced the weaker the ligand donor strength is; i.e., the methyl substitution can partially compensate for the smaller electron-releasing property of weaker donors. It should be noted, however, that eq 4 overestimates the stabilization, since the energy difference of both planar forms of the free crotyl anion, i.e., 3.0 kcal/mol in favor of the anti form, is included. But even if this is taken into account, the calculations indicate a stronger Ni-π-butenyl coordination due to the α-alkyl substituent.

The migration of electron density toward the crotyl part (cf. Table 10) follows the same trends that are observed for the allyl complexes **I** and **III**. However, the charge distribution among the allylic carbons C^1 and C^3 is unsymmetrical, with the electron density preferentially located at C^1 rather than at the methyl substituted C^3 center. The entire negative charge of the butenyl group is predicted to be larger for the allyl complexes than for the corresponding crotyl complexes. In addition to the stronger coordination this may be explained by an enhanced crotyl → Ni donating interaction, supported by the electron-releasing property of the methyl substituent.

Table 9. Calculated Potential-Energy (with and without ZPC) and Gibbs Free Energy Profile for the Isomerization of the Butenyl Group in Cationic [Ni(butenyl)(butadiene)L]$^+$ (I, II), Ni(butenyl)(ethylene)(butadiene)L]$^+$ (V) and Neutral [Ni(butenyl)(butadiene)I] (III, IV), [Ni(butenyl)(ethylene)(butadiene)I] (VI) Complexes (kcal/mol)[a,b]

		η^1-σ-butenyl	
	η^3-π-butenyl	TS-A[c]	TS-B[c]
[Ni(allyl)(butadiene)L]$^+$			
Ia (L = PF_3)	0.0 (0.0) *0.0*		30.2 (28.6) *28.4*
Ib (L = PH_3)	0.0 (0.0) *0.0*		25.6 (24.2) *23.4*
Ic (L = PMe_3)	0.0 (0.0) *0.0*		23.3 (22.1) *21.4*
Id (L = C_2H_4)	0.0 (0.0) *0.0*		25.2 (23.2) *22.1*
[Ni(allyl)(butadiene)I]			
III	0.0 (0.0) *0.0*	20.6 (19.3) *17.8*	19.2 (18.2) *16.7*
[Ni(crotyl)(butadiene)L]$^+$			
IIa (L = PF_3)	syn 0.0 (0.0) *0.0* anti 3.0 (3.0) *3.0*		35.9 (33.9) *32.2*
IIb (L = PH_3)	syn 0.0 (0.0) *0.0* anti 2.8 (2.8) *2.9*		31.4 (29.8) *28.5*
IIc (L = PMe_3)	syn 0.0 (0.0) *0.0* anti 4.6 (4.9) *5.3*		31.5 (30.3) *29.9*
IId (L = C_2H_4)	syn 0.0 (0.0) *0.0* anti 3.6 (3.6) *3.6*		30.1 (28.5) *28.0*
[Ni(crotyl)(butadiene)I]			
IV	syn 0.0 (0.0) *0.0* anti 3.0 (2.8) *2.6*	24.9 (23.6) *22.3*	24.3 (22.9) *21.5*
[Ni(crotyl)(ethylene)(butadiene)L]$^+$			
Va (L = PF_3)		24.9 (25.4)	25.5 (26.6)
Vb (L = PH_3)		23.9 (24.4)	24.7 (26.2)
Vc (L = PMe_3)		25.8 (26.8)	29.0 (30.3)
Vd (L = C_2H_4)		25.8 (26.5)	27.3 (28.0)
[Ni(crotyl)(ethylene)(butadiene)I]			
VI		22.5 (23.1)	26.7 (27.3)

[a] Numbers in parentheses include the zero point corrections, while those in italics are the Gibbs free energies. [b] Concerning **V** and **VI**, which were built in a bimolecular reaction, only ΔE and ΔE+ZPC are given. [c] For an explanation, see the text.

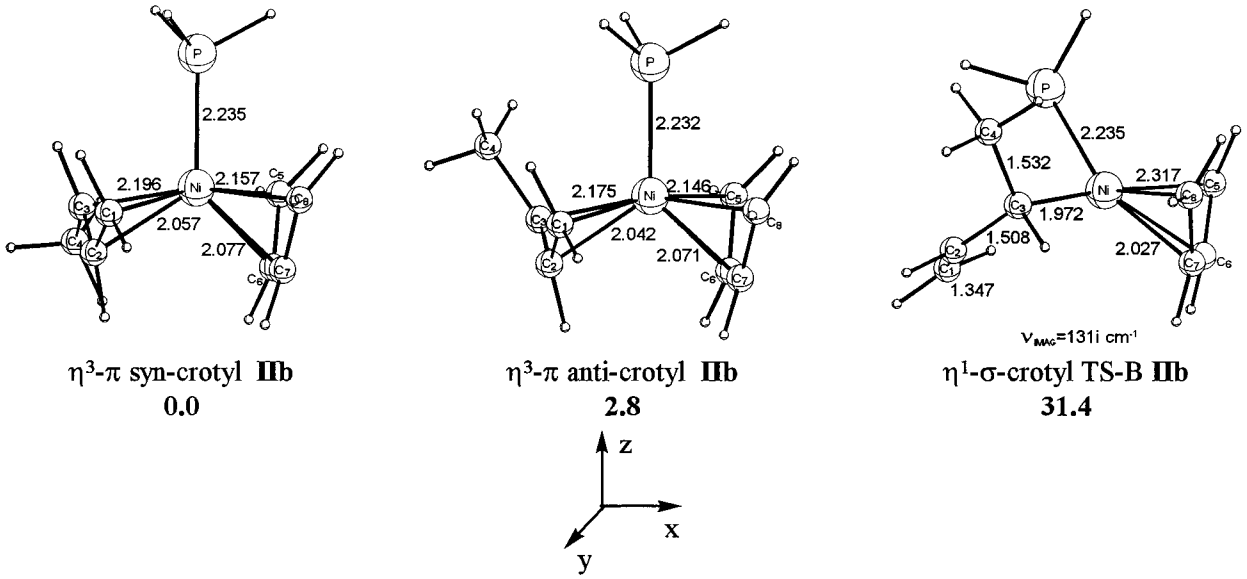

η^3-π syn-crotyl **IIb** 0.0 | η^3-π anti-crotyl **IIb** 2.8 | η^1-σ-crotyl TS-B **IIb** 31.4

Figure 9. Selected geometric parameters of the optimized structures (Å) for the rotational automerism of the allyl group in [Ni(crotyl)(butadiene)-L/I]$^{(+)}$ complexes together with relative energies (ΔE in kcal/mol).

2. η^1-σ-Crotyl Complexes. Similar to the rotational automerization of the allyl group, the anti-syn isomerization of the crotyl group preferentially takes place via TS-B (cf. Table 9). The competitive outward rotation is unlikely for **II**, because the rotation around C^2-C^3 is hindered. Regarding **IV**, TS-A lies 0.6 kcal/mol (ΔE) above TS-B. In all cases both enantiomorph forms of TS-B differ by less than 1.0 kcal/mol. The isomer with the methyl group pointing toward the ligand is energetically favored.

The free energy barrier to isomerizing the crotyl group (cf. Table 9), commencing from the more stable *syn*-η^3-π form, is 32.2 kcal/mol (**IIa**), 28.5 kcal/mol (**IIb**), 29.9 kcal/mol (**IIc**), 28.0 kcal/mol (**IId**), and 21.5 kcal/mol (**IV**). Thus, the barrier is about 4−8 kcal/mol higher due to a methyl substitution on C^3.

The changes of the crotyl group's charge distribution upon $\pi \rightarrow \sigma$ rearrangement is very similar to that observed in **I** and **III**. For ligand complexes of essential donor type, such as **IIa-c** and **IV**, we find that the larger the overall negative charge of the crotyl moiety, the smaller the amount of energy required for isomerization. The migrated negative charge is similar for PR_3 ligands (0.13 electrons for **IIa**,**b** and 0.11 electrons for **IIc**) and

Table 10. Charges in Cationic [Ni(crotyl)(butadiene)L]$^+$ (II) and Neutral [Ni(crotyl)(butadiene)I] (IV)[a]

	C^1H_2	C^2H	C^3H	C^4H_3	Σ_{crotyl}	$\Sigma_{butadiene}$	L/I	Ni
η^3-π *syn*-crotyl								
IIa (L = PF_3)	0.028	−0.038	0.038	0.082	0.110	0.008	0.245	0.637
IIb (L = PH_3)	0.000	−0.040	0.012	0.067	0.040	−0.063	0.274	0.749
IIc (L = PMe_3)	−0.015	−0.038	−0.008	0.061	−0.001	−0.116	0.357	0.760
IId (L = C_2H_4)	0.015	−0.044	0.064	0.075	0.111	0.036	−0.008	0.861
IV	−0.021	−0.080	0.003	0.027	−0.070	−0.182	−0.546	0.798
η^1-σ-crotyl TS-B[b]								
IIa (L = PF_3)	0.016	0.004	−0.097	0.059	−0.018	0.100	0.297	0.620
IIb (L = PH_3)	0.006	0.003	−0.138	0.038	−0.091	0.061	0.323	0.707
IIc (L = PMe_3)	0.001	0.000	−0.141	0.029	−0.112	0.007	0.391	0.714
IId (L = C_2H_4)	0.022	−0.002	−0.064	0.053	0.009	0.094	0.026	0.871
IV	−0.001	−0.019	−0.163	0.016	−0.166	−0.099	−0.472	0.737

[a] Based on natural population analysis; for atom labels, see Figure 9. [b] For an explanation see the text.

somewhat smaller (0.10 electrons) for **IId** and **IV** (cf. Table 10). Overall the charge accumulation within the butenyl moiety is smaller for the crotyl than for the corresponding allyl complexes, which is due to the donating ability of the methyl group.

Similar to reaction 4, the stability of TS-B, influenced when going from allyl to crotyl, is evaluated utilizing reaction 5 (cf. Table 8).

$$[(\eta^1\text{-}\sigma\text{-}C_3H_5)(\eta^4\text{-}C_4H_6)\text{Ni-L/I}]^{(+)}\ (\text{TS-B}) + \text{rotated}\ [C_4H_7]^-\ (\text{TS-B}) \rightarrow [(\eta^1\text{-}\sigma\text{-}C_4H_7)(\eta^4\text{-}C_4H_6)\text{Ni-L/I}]^{(+)}\ (\text{TS-B}) + \text{rotated}\ [C_3H_5]^-\ (\text{TS-B}) \quad (5)$$

In contrast to the stabilizing effect for the π-crotyl form, the methyl substituent, in general, destabilizes the σ-crotyl rotational transition structure. According to the charge distribution given in Table 10, from an electronic point of view, no clear indication that may explain the different extent of reduced stabilization is obvious. We therefore believe in a destabilization of at most about 2 kcal/mol due to a purely electronic contribution. The decreased stability predicted for **IIc** and **IV** may therefore be attributed to steric interactions, probably due to the interaction of the methyl substituent with the ligand. The steric congestion during the formation of TS-B is estimated at about 3 kcal/mol (**IIc**) and 1 kcal/mol (**IV**), respectively, based on the relative stabilities predicted according to eq 5.

For cationic and neutral [Ni(butenyl)(butadiene)-L/I]$^{(+)}$ complexes the activation energy to isomerize the butenyl group increases due to the α-alkyl substituent on the butenyl group. Both the stabilization of the π-butenyl form and the destabilization of the σ-butenyl form give rise to the higher barrier. For modest donor ligands (**IIa**, **b**, and **d**) the calculations suggest that the enhanced π-butenyl stability is mainly responsible for the increased activation barrier, whereas to a similar extent both effects contribute to the barrier in the case of strong donors (**IIc** and **IV**). If only electronic reasons are considered, however, the barrier is estimated to increase by about 5 kcal/mol, due to the more stable π-butenyl form, for all ligands investigated. The calculations indicate, however, that the barrier is probably also affected by steric interactions. With increasing ligand bulkiness the stability of the σ-butenyl form is much more affected than the stability of the π-butenyl form, which is due to more unfavorable steric interactions of the butenyl chain with the cis ligand within the quasi planar coordination plane. Therefore, the formation of the σ-butenyl rotational transition structure is hampered by sterically demanding ligands, thus giving rise to an increased barrier, although they attenuate the anti π-butenyl form, as well. Concerning the rather mildly demanding PMe_3 ligand, the steric contribution can be estimated to be about 3 kcal/mol. If PPh_3 or much more bulky ligands are concerned it can be expected that the barrier could be essentially determined by increased steric interactions in the course of $\pi \rightarrow \sigma$ butenyl conversion.

E. Cationic [Ni(crotyl)(ethylene)(butadiene)L]$^+$ (L = PF_3, PH_3, PMe_3, C_2H_4) and Neutral [Ni(crotyl)-(ethylene)(butadiene)I] Complexes. Now the effect of an additional ethylene ligand that occupies the single vacant site on the Ni(II) center arising during the $\pi \rightarrow \sigma$ butenyl group conversion, will be inspected. Since the energetically preferred formal 18-electron configuration is preserved, the σ-butenyl form is stabilized, which shifts the isomerization barrier down. On the other hand the stability of the π-butenyl group in 18-electron five-coordinate Ni(II) complexes will not be affected by an additional ligand, as long as the ligand does not have the capability to expel another ligand by ligand exchange. This however will not be considered in the present study. Thus attention will be focused on the σ-butenyl rotational transition structures only. Those are denoted as follows: [Ni(σ-C_4H_7)(C_4H_6)(C_2H_4)L]$^+$, **V**, and [Ni(σ-C_4H_7)(C_4H_6)(C_2H_4)I], **VI**, with the neutral ligands labeled in the same manner as in section C. The π-butenyl complexes are those already investigated in the previous section, **II** and **IV**.

1. Cationic [Ni(η^1-σ-crotyl)(ethylene)(butadiene)L]$^+$ (L = PF_3, PH_3, PMe_3, C_2H_4) and Neutral [Ni(η^1-σ-crotyl)(ethylene)(butadiene)I] Complexes. For the σ-butenyl rotational transition structures a trigonal bipyramidal coordination sphere around the Ni-(II) center was determined to be the most stable. The strongest donor is the axial position σ-butenyl. The equatorial positions are taken by the two ligands, and butadiene is prone[11] coordinated. Thus, butadiene may occupy an equatorial and an axial position.

In both isomers of the rotational transition structures, which were passed through for the outward (TS-A) and the inward (TS-B) rotation, the free rotation around the C^2-C^3 bond is not hindered. In addition to the two enantiomorph forms possible for each of the TS-A and TS-B, several σ-butenyl structures were located, all of them true transition states for anti-syn isomerization. They differ with regard to the mutual orientation of the

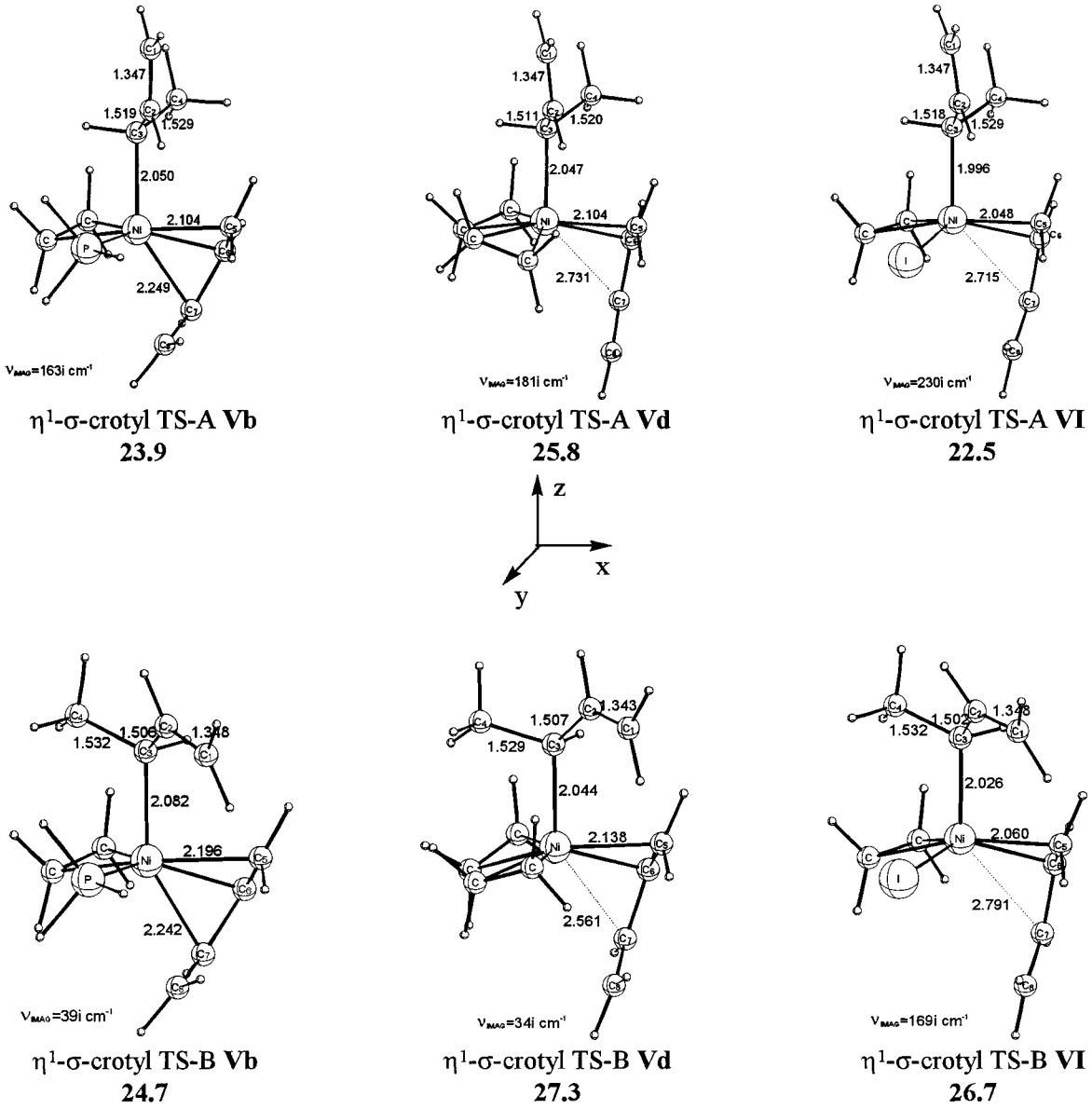

Figure 10. Selected geometric parameters of the optimized rotational transition structures (Å) for the isomerization of the crotyl group in [Ni(crotyl)(ethylene)(butadiene)-L/I]$^{(+)}$ complexes together with relative energies (ΔE in kcal/mol).

equatorial ligands and also with the rotation around the Ni−C^3 bond. The most stable σ-butenyl transition structures, **Vb**, **Vd**, and **VI**, which were obtained after an extensive search, are displayed in Figure 10.

The bonding of the σ-butenyl group (cf. Figure 11) mainly arises from the interaction of the free electron pair with the formally vacant Ni d_{zz} orbital (Figure 11a). The equatorial ligands interact via their HOMO's, i.e., sp_σ lone pair (I^-, PR_3) and π orbital (C_2H_4), with the empty Ni d_{zz} and s orbitals (Figure 11b). There is no clear indication for a back-donation interaction in the case of PR_3 ligands and iodine anion. On the other hand, the ethylene π^* acceptor orbital preferably interacts with the Ni d_{xx-yy} orbital (Figure 11c). This explains the in-plane coordination, with regard to the equatorial *xy* plane, of ethylene, as predicted for all σ-butenyl complexes. Considering the prone coordination, butadiene may interact in two different ways. On the one hand, the equatorial C^6═C^7 double bond is coordinated in a very similar fashion to that described for ethylene. For the C^8═C^9 double bond there is a donating interaction with the Ni d_{zz} orbital, but a back-donation is not possible (Figure 11d). For a strong bonding interaction, butadiene has to compete with the others ligands. Therefore, depending on the ligand donor strength, butadiene is coordinated either monodentate (i.e., η^2-mode for iodine anion) or bidentate (i.e., intermediate η^3-mode for PR_3).

The outward rotation through TS-A is the pathway where the anti−syn isomerization probably takes place. To proceed along the alternative route via TS-B a higher energy of about 1 kcal/mol (**Va**,**b**,**d**), 3 kcal/mol (**Vc**), or 4 kcal/mol (**VI**), respectively, is necessary. The energy gap between both transition states roughly increases the more sterically interacting the ligand is, which supports the assumption that the inward rotation is unfavorable due to stronger steric interactions with the equatorial ligands. For the σ-C^3 intermediates (cf. Figure 2), with L = PMe_3, the internal rotation around the Ni−C^3 σ-bond is energetically more feasible than that around the C^2−C^3 bond (via TS-A), which is estimated to about 1.9 kcal/mol.

Table 11. Charges in Cationic [Ni(η^1-σ-crotyl)(ethylene)(butadiene)L]$^+$ (V) and Neutral [Ni(η^1-σ-crotyl)(ethylene)(butadiene)I] (VI)[a]

	C^1H_2	C^2H	C^3H	C^4H_3	Σ_{crotyl}	$\Sigma_{butadiene}$	$\Sigma_{ethylene}$	L/I	Ni
η^1-σ-crotyl TS-A[b]									
Va (L = PF_3)	0.104	−0.078	−0.071	0.049	0.003	0.101	−0.007	0.238	0.664
Vb (L = PH_3)	0.087	−0.077	−0.093	0.040	−0.042	0.034	−0.034	0.276	0.765
Vc (L = PMe_3)	0.075	−0.076	−0.105	0.037	−0.069	−0.011	−0.048	0.347	0.781
Vd (L = C_2H_4)	0.098	−0.072	−0.004	0.057	0.080	0.044	−0.016	0.0	0.892
VI	0.011	−0.015	−0.073	0.011	−0.066	−0.094	−0.116	−0.553	0.820

[a] Based on natural population analysis; for atom labels, see Figure 10. [b] For an explanation, see the text.

Commencing from the *syn*-η^3-butenyl complexes **II** and **IV**, respectively, the activation energy for isomerization (ΔE) is 24.9 kcal/mol (**Va**), 23.9 kcal/mol (**Vb**), 25.8 kcal/mol (**Vc**), 25.8 kcal/mol (**Vd**), and 22.5 kcal/mol (**VI**) (cf. Table 9). It is interesting to observe similar barriers for **V** and a reduced energy gap to **VI**, which is due to the additional ethylene ligand. The calculations indicate a pronounced stabilization of the σ-butenyl transition structure by the coordination of an additional ethylene ligand. The isomerization barrier (ΔE) decreases by 11.0 kcal/mol, 7.5 kcal/mol, and 5.7 kcal/mol for L = PF_3, PH_3, and PMe_3, respectively; by 4.3 kcal/mol for L = C_2H_4; and by only 1.8 kcal/mol for iodine anion. For the PR_3 ligands, the σ-butenyl form is found to be more stabilized as ligands become less basic, which gives rise to similar barriers.

This can be understood from the ambivalent nature of ethylene (cf. Table 11). On the one hand, its donating ability is decisive, which may compensate for the weaker basicity of PF_3, thus enabling the increase in the amount of accumulated negative charge in the butenyl moiety which is necessary in order to shift down the barrier. In combination with the more strongly basic PMe_3 ligand, the alkyne π-acidity prevails, which may restrict the partial negative charge of the butenyl group to a certain degree. We believe the additional ethylene ligand influences the stability of the σ-butenyl form in two ways. First, the stability increases upon coordination, and secondly the stability can be enhanced further by the ligand donor strength, depending on the other ligand's electron-releasing property.

For PR_3 ligands, the magnitude of the migrated negative charge decreases (0.11, 0.08, and 0.07 electrons for **Va**, **b**, and **c**, respectively) as the ligand donor strength increases. The slightly higher barrier for **Vc** can probably be attributed to steric effects. Sterically interacting ligands should hamper the formation of the trigonal bipyramidal σ-butenyl structure to a lesser extent than the formation of the quasi planar [Ni(σ-butenyl)(butadiene)L/X]$^{(+)}$ structure. Therefore, the steric interaction is estimated to enlarge the barrier by at most about 2.0 kcal/mol on the basis of the estimates made in the previous section. Taking this into account, the isomerization barriers are very similar, from an electronic point of view, for all PR_3 ligands investigated. The smallest stabilization affected by the additional ethylene ligand is calculated for the strongest donor, the iodine anion. This agrees with the findings, that in this case a migration of electron density toward the butenyl group does not occur (cf. Table 11).

Conclusions

The transition-metal assisted isomerization of the butenyl group, which is a key step in the entire course of butadiene polymerization and most likely takes place via $\pi \rightarrow \sigma$ butenyl conversion followed by internal rotation around the C^2-C^3 single bond, was examined theoretically by applying density functional theory in cationic and neutral (butenyl)(butadiene)(monoligand)-nickel(II) complexes. The influence of the following effects were studied: the donor−acceptor ability of a neutral or anionic ligand; a methyl substitution of the butenyl group at the terminal C^3 atom that is involved in the rotation; and the substitution of an additional ethylene ligand. The effects were investigated in a detailed manner with respect to their influence on the geometry of η^3-π reactants and products; the corresponding η^1-σ rotational transition structures; and also on the rotational barrier height. For the neutral ligand L = PF_3, PH_3, PMe_3, and C_2H_4 was chosen, whereas the iodine anion is adopted as a realistic anionic ligand X.

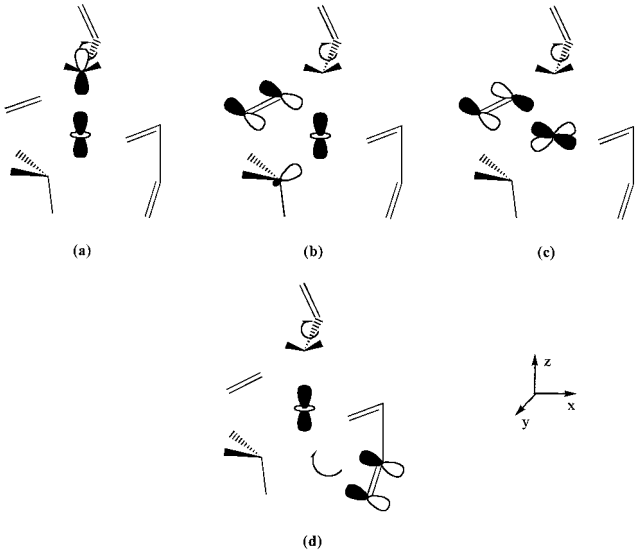

Figure 11. Important orbital interactions in [Ni(σ-butenyl)(ethylene)(butadiene)-L/I]$^{(+)}$ complexes, schematic sketched concerning L = PR_3.

During the process of rotational isomerism the important structural accommodation is the pyramidalization of the carbon center associated with sp^3 hybridization. There are two conformers of the rotational transition structure for the inward and outward rotation of the electron pair which is formed during the rotation. The $\pi \rightarrow \sigma$ butenyl conversion followed by formation of the rotational transition structure is accompanied by negative charge migration, which is mainly located at the rotated sp^3 carbon atom.

The geometries of the planar and rotated forms of the free allyl and 1-methylallyl (crotyl) anions and also the rotational barriers are calculated in close agreement with previous theoretical studies.[19a−c] Commencing from the most stable planar isomer, the activation energy

along the favored inward rotation is 1.1 kcal/mol higher for the crotyl anion than for the allyl anion.

The reliability of the chosen computational approach was judged by the investigation of the experimentally well-investigated rotational automerization of one allyl group in the [bis(allyl)-Ni-PMe_3] complex. The calculated geometric parameters are in excellent agreement with X-ray data using a standard DZVP (basis-I) basis. Both LDA/BP and B3LYP levels of computation are a good choice for predicting the geometric parameters to a highly accurate degree, but only the LDA/BP level can be deemed satisfactory for predicting the automerization barrier, since at the B3LYP level the barrier height is significantly underestimated.

The rotational isomerism in cationic and neutral (butenyl)(butadiene)(monoligand)nickel(II) complexes starting from tetragonal pyramidal π-butenyl complexes with the η^3-butenyl and η^4-butadiene moieties in supine−supine arrangement proceeds through distorted square-planar η^1-σ-butenyl complexes. As a consequence of the $\pi \rightarrow \sigma$ butenyl conversion, the rotational transition states are characterized by an empty coordination site on the metal. The rotational isomerism preferably takes place via inward rotation. The energy required for isomerization strongly depends on the ligand's donor−acceptor ability. For donor ligands (PR_3 and the iodine anion), the activation energy is essentially determined by their donating ability. The free-energy rotational barrier of the allyl group decreases in the following order: PF_3 (28.4 kcal/mol) > PH_3 (23.4 kcal/mol) > PMe_3 (21.4 kcal/mol) > I^- (16.7 kcal/mol), while the ligand donor strength increases, due to a pronounced stabilization of the σ-allyl rotational transition structure by strong donors. This is supported by the migration of electron density toward the butenyl group. The entire butenyl part's effective negative charge correlates with the stabilization of the σ-allyl structure. As opposed to these donor ligands, ethylene supports the formation of the σ-allyl form by its π-acidity, due to an increased back-donation into the olefinic π^*-orbital upon $\pi \rightarrow \sigma$ conversion.

The activation energy for isomerization increases by about 4−8 kcal/mol due to an α-alkyl C^3-substitution of the butenyl chain. Both the stabilization of the π-butenyl form and the destabilization of the σ-butenyl form give rise to the higher barrier. For modest donor ligands (PF_3, PH_3, and C_2H_4) the calculations indicate that the enhanced π-butenyl stability is mainly responsible for the increased activation barrier, whereas both effects contribute to the barrier in the case of strong donors (PMe_3, I^-). If only electronic factors are considered, however, the barrier is estimated to enlarge by about 5 kcal/mol, due to the amplified π-butenyl coordination, for all ligands investigated. There are, however, indications that the barrier is probably also affected by steric factors, which attenuate the σ-butenyl form much more than the π-butenyl form due to unfavorable steric interactions of the butenyl group with the cis ligand.

With increasing ligand bulkiness it can be expected that the barrier could be essentially determined by enhanced steric interactions upon $\pi \rightarrow \sigma$ conversion.

The σ-butenyl transition structure is stabilized by the occupation of its single vacant site by an additional ethylene ligand. A trigonal bipyramidal coordination sphere around Ni(II) was determined as the most stable, with one of the axial positions occupied by the σ-butenyl group and butadiene in prone coordination. Depending on the ligand's donating ability, butadiene is coordinated either monodentate (iodine anion) or bidentate (PR_3 ligands). Due to smaller steric interactions with the equatorial ligands the outward rotation is the pathway where the anti−syn isomerization preferentially takes place. The calculations indicate a pronounced stabilization of the σ-butenyl transition structure. For PR_3 ligands the σ-butenyl form is found to be the more stabilized the weaker basic the ligands are. That gives rise to very similar free energy barriers of about 24−26 kcal/mol. Additionally, the activation energy gap between neutral and anionic ligands decreases under the influence of the additional ligand. This can be understood from the ambivalent nature of ethylene. On the one hand, its donating ability is decisive which may compensate for weaker basicity of such ligands as PF_3. In combination with stronger basic ligands, such as PMe_3, its π-acidity prevails, which may restrict the partial negative charge of the butenyl group to a certain degree. Sterically interacting ligands should hamper the formation of the trigonal bipyramidal σ-butenyl structure to a lesser extent than formation of the quasi planar [Ni(σ-butenyl)(butadiene)L/X]$^{(+)}$ structure.

The balance between the rate of the pre-established anti−syn isomerization equilibrium and the rate of the butadiene insertion, which may determine the cis−trans regulation of polymer formation, will be discussed in detail in subsequent papers for monoligand and "ligand-free" Ni(II) complexes.

Acknowledgment. This work is supported by the Bundesministerium für Bildung und Forschung (BMBF). One of the authors (S.T.) is indebted to Prof. R. Ahlrichs (University of Karlsruhe) for making the latest version of TURBOMOLE available. We acknowledge excellent service by the computer centers HLRZ Jülich, ZIB Berlin, and URZ Halle.

Supporting Information Available: Tables of Cartesian coordinates of selected optimized structures. This material is available free of charge via the Internet at http://pubs.acs.org.

OM9810302